



King Saud University
College of Computer and Information Sciences
Department of Computer Engineering

PN Acquisition Using Adaptive Thresholding and Smart Antenna for Direct Sequence CDMA Mobile Communication

**Submitted in Partial Fulfillment of the Requirements for the
Master's Degree in the Department of Computer Engineering at
the College of Computer and Information Sciences,
King Saud University**

By

Nour Nasser Alhariqi

**24 Safar 1434
6 January 2013**

**PN Acquisition Using
Adaptive Thresholding and
Smart Antenna for Direct Sequence
CDMA Mobile Communication**

By

Nour Nasser Alhariqi

Approved on 24 Safar 1434

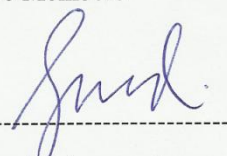
6 January 2013

Supervisor

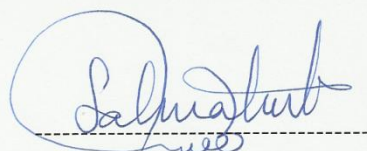


Professor Mourad Barkat

Committee Members



Dr. Ghulam Muhammad



Dr. Salman Alqahtani

ملخص الرسالة

الكلية: كلية علوم الحاسب والمعلومات – جامعة الملك سعود

القسم: قسم هندسة الحاسب الآلي

المسار: مسار الشبكات

عنوان الرسالة: مزامنة شفرات الـ PN باستخدام العتبة التكيفية والهوائي الذكي لاتصالات التسلسل

المباشر/الوصول المتعدد بتقسيم الشفرات المتنقلة.

اسم الطالب: نور ناصر الحريقي

اسم المشرف: الأستاذ الدكتور مراد بركات

الدرجة العلمية: الماجستير

تاريخ المناقشة: ٢٤ صفر ١٤٣٤ هـ

الكلمات الدلالية للبحث: مزامنة شفرات الـ PN ، العتبات التكيفية ، الهوائيات الذكية ، اتصالات التسلسل

المباشر/الوصول المتعدد بتقسيم الشفرات المتنقلة.

الملخص:

هذه الرسالة تقدم آلية فعالة لعملية المزامنة التسلسلية أحادية الـ dwell لشفرات الـ PN وذلك بأنظمة اتصالات التسلسل المباشر/الوصول المتعدد بتقسيم الشفرات (DS-CDMA) لقنوات اتصال Rayleigh متعددة المسارات ذات الاضمحلال البطيء. في المرجع [١]، صفوان و بركات قدموا طريقة مبتكرة تتبنى استخدام الهوائيات الذكية مع العتبة التكيفية معدل الإنذار الخاطئ الثابت (CFAR) في عملية مزامنة شفرة الـ PN في أنظمة الاتصالات ذات النطاق العريض.

في هذا العمل البحثي، نظام الاتصالات المقترح لازال يتبنى فكرة استخدام الهوائيات الذكية في عملية المزامنة التسلسلية لشفرة الـ PN ولكن بتطبيق خوارزمية الـ CMLD-CFAR كعتبة تكيفية في البيانات ذات اشارات المستخدمين المتعددة. تتميز بيانات الاتصال المتنقل بوجود الاشارات المتعددة المسارات و اشارات المستخدمين الآخرين والتي لها تأثير على اداء عملية مزامنة شفرة الـ PN . استخدام آليات العتبة الثابتة في عملية المزامنة يتميز

بعدم القدرة على التكيف مع تلك البيئات المتغيرة. ونتيجة لذلك سيكون هناك إزدياد في معدل الإنذار الخاطئ و/أو انخفاض في احتمالية الكشف وبناء عليه فإن استخدام العتبات التكيفية مطلب ضروري. الهوائيات الذكية هي مصفوفة من عناصر الهوائيات التي بإمكانها تعديل نمط المصفوفة تكيفيا لتقليل تأثير الضوضاء وتداخلات الوصول المتعدد (MAI) من المستخدمين الآخرين والاشارات المتعددة المسارات.

تم تحليل الآلية المقدمة لتزامن شفرات الـ PN بإستنتاج المعادلات الرياضية لاحتمال الإنذار الخاطئ، احتمال الكشف، المتوسط الزمني للتزامن. نتائج المحاكاة المقدمة توضح متانة وفاعلية نظام مزامنة شفرة الـ PN المقدم لنظام الاتصالات المعتبر.

Abstract

College: Collage of Computer and Information Sciences – King Saud University

Department: Department of Computer Engineering

Track: Network track

Title of the thesis: PN Acquisition Using Adaptive Thresholding and Smart Antenna for Direct Sequence CDMA Mobile Communication

Student Name: Nour Nasser Alhariqi

Supervisor Name: Professor Mourad Barkat

Degree: Master

Discussion Date: 6 January 2013

Tagged to search: PN code acquisition, Smart antenna, CFAR, DS-CDMA

Abstract :

This thesis presents an efficient single dwell serial search pseudo-noise (PN) code acquisition scheme for direct sequence code division multiple access (DS-CDMA) communication systems in Rayleigh slowly fading multipath channel. In [1], Sofwan and Barkat presented a novel approach using smart antenna and adaptive thresholding constant false alarm rate (CFAR) for PN code acquisition in wideband communication.

In this thesis, the proposed communication system still considers PN code acquisition by using smart antenna but with the censored mean level detector constant false alarm rate (CMLD-CFAR) as an adaptive threshold processor in multiuser signals situations. In mobile communication environments, multipath signals and other users' signals affect the performance of PN code acquisition. Fixed threshold techniques are unable to adapt to these varying environments. Accordingly, a high false alarm rate

and/or a low detection probability may result, and thus adaptive thresholding techniques are essential. A smart antenna is an array of antenna elements that can modify the array pattern adaptively to minimize the effect of noise, multiple access interference (MAI) of other users, and multipath fading.

The proposed PN code acquisition scheme has been analyzed by deriving closed form expressions for the probability of false alarm, the probability of detection, and the mean acquisition time. The simulation results presented show the robustness and efficiency of the acquisition process in the communication system considered.

Acknowledgements

First and foremost, I would like to express my deepest gratitude to Allah Almighty for providing me the blessings to complete this work. All praise is to Allah.

My sincere gratitude and thanks goes to Professor Mourad Barkat for his supervision, patience, and support during my thesis work. I am eternally grateful to him, because with his guidance, enthusiasm and encouragement, my dream of writing and publishing a paper became a reality. Truly, I am very proud that Professor Mourad is my mentor.

Also I am most grateful to my colleague Aghus Sofwan for his continuous and unbounded help, the brilliant discussions, and for sure his patience to my frequent questions. I cannot imagine that I can find a colleague more collaborative than him. So here, I would like to express my greatest admiration and a lot of thanks to Aghus.

My thanks also extend to the members of my thesis committee: Dr. Ghulam Muhammad and Dr. Salman Alqahtani.

My loving thanks are for my wonderful mother for her prays, endless love, priceless friendship, support and continues encouraging. Also, I express my deepest sense of gratitude to my great father for what he did and does for me. My warmest thanks also go to my brothers: Mohammad, Ahmad, Qusai, Suhaip, and Qutaibah for the love that they grant me. They are always standing beside me and supporting me during the entire period of my graduate studies.

Table of Contents

ملخص الرسالة.....	- iii -
Abstract.....	- v -
Acknowledgment.....	- vii -
List of Figures.....	- x -
List of Abbreviations.....	- xii -
Chapter 1 – General Introduction.....	- 1 -
1.1 Introduction	- 2 -
1.2 Literature Review.....	- 4 -
1.3 Objectives	- 9 -
1.4 Organization of the Thesis	- 11 -
Chapter 2 – Spread Spectrum Communication, Adaptive Thresholding CFAR Detection, and Smart Antenna.....	- 12 -
2.1 Introduction	- 13 -
2.2 Spread Spectrum.....	- 14 -
2.2.1 What is the Spread Spectrum?	- 15 -
2.2.2 Pseudo Noise Code Sequences	- 16 -
2.2.3 Types of Spread Spectrum.....	- 16 -
2.3 Code Division Multiple Access	- 19 -
2.4 PN Code Acquisition for Direct Sequence Receiver	- 22 -
2.5 Adaptive Thresholding CFAR Detection	- 27 -
2.5.1 Adaptive CFAR Detection	- 27 -
2.5.2 Adaptive CFAR thresholding for the PN code acquisition	- 34 -
2.6 Smart Antenna Systems	- 34 -
2.6.1 What is the Smart Antenna System?.....	- 35 -
2.6.2 Architecture of the Smart Antenna System	- 36 -
2.6.3 Adaptive Beamforming Algorithms.....	- 38 -
2.6.4 Types of the Smart Antenna Systems	- 39 -
2.6.5 The Advantages of the Smart Antenna Systems.....	- 43 -
Chapter 3 – Communication System Model and Analysis.....	- 45 -
3.1 Introduction	- 46 -

3.2	Communication System Model	- 47 -
3.2.1	The Transmitted Signal	- 48 -
3.2.2	The Communication Channel Model	- 49 -
3.2.3	The Antenna Array Elements	- 50 -
3.2.4	The Received Signal	- 50 -
3.2.5	The Correlator.....	- 51 -
3.2.6	The Least Mean Square Processor.....	- 53 -
3.2.7	The CMLD-CFAR Processor	- 54 -
3.3	System Analysis.....	- 55 -
3.3.1	The Probability of False Alarm	- 56 -
3.3.2	The Probability of Detection	- 58 -
3.3.3	The Mean Acquisition Time.....	- 59 -
3.4	Results and Discussions	- 63 -
3.4.1	Probability of Detection	- 64 -
3.4.2	Mean Acquisition Time.....	- 70 -
	Chapter 4 – Conclusion.....	- 73 -
4.1	Summary and Conclusions	- 74 -
4.2	Suggestions for Future Research Work.....	- 75 -
	Appendix - MATLAB Codes.....	- 76 -
	References.....	- 83 -

List of Figures

Fig. 2-1: The multiple access techniques: (a) FDMA, (b) TDMA, and (c) CDMA.....	14
Fig. 2-2: Spread spectrum system.....	15
Fig. 2-3: Direct sequence spreading operation.....	17
Fig. 2-4: Direct sequence despreading operation.	18
Fig. 2-5: Frequency hopping spread spectrum.	19
Fig. 2-6: DS-CDMA.	19
Fig. 2-7: DS-CDMA transmitter.	20
Fig. 2-8: Non-coherent DS-CDMA receiver.	22
Fig. 2-9: Coherent DS-CDMA receiver.	22
Fig. 2-10: A classification of the PN code acquisition schemes based on the detector structure.	26
Fig. 2-11: Effect of the noise power increase on the probability of false alarm for a fixed threshold.	28
Fig. 2-12: Cell averaging CFAR.....	29
Fig. 2-13: Model of a clutter edge where test cell in clear.....	30
Fig. 2-14: Model of a clutter edge where test cell in clutter.	30
Fig. 2-15: Threshold too high.	32
Fig. 2-16: Threshold not high enough.	32
Fig. 2-17: The clutter edge and spikes model.	33
Fig. 2-18: Adaptive PN code acquisition detector.....	34
Fig. 2-19: Human auditory function.....	36
Fig. 2-20: Reception part of the smart antenna system.....	37
Fig. 2-21: Transmission part of a smart antenna.....	38
Fig. 2-22: Coverage pattern (a) Switched beam (b) adaptive array	40
Fig. 2-23: Switched beam smart antenna system.	40
Fig.2-24: Switched beam and adaptive array beams in the presence of interference signals.	42
Fig.2-25: Switched beam and adaptive array coverage in low/significant interference environment.	42
Fig. 3-1: Block diagram of the proposed system.....	48

Fig. 3-2: Tapped delay line model of the frequency-selective channel.....	49
Fig. 3-3: Correlator consists of in-phase (I) and quadrature-phase (Q) components.....	51
Fig. 3-4: The LMS processor.....	53
Fig. 3-5: CMLD-CFAR processor.	55
Fig. 3-6: The circular state transition diagram.....	60
Fig. 3-7: The H_I state..	62
Fig. 3-8: Comparison of P_d using CA-CFAR processing with CMLD-CFAR system with multipath.	65
Fig. 3-9: Comparison of P_d between the proposed system with $M = 1$ and 2 and the APP system.	66
Fig. 3-10: Effect of the number of antenna elements M on the detection performance....	67
Fig.3-11: Comparison of P_d for different number of antenna elements M and different values of number of censored cells k	68
Fig. 3-12: Effect of the number of reference cells N_c on the detection performance.....	69
Fig. 3-13: Effect of the correlation length integer R on the detection performance.....	70
Fig. 3-14: Effect of the number of antenna elements M on the T_{acq}	71
Fig. 3-15: Effect of the correlation length integer R on the T_{acq}	72

List of Abbreviations

AAP	adaptive acquisition processor
AWGN	additive white Gaussian noise
A/D	analog-to-digital
ASIC	application specific integrated circuits
BPSK	binary PSK
CUT	cell under test
CA-CFAR	cell-averaging constant false alarm rate
CMLD	censored mean level detector
CMLD-CFAR	censored mean level detector constant false alarm rate
CDMA	code division multiple access
CFAR	constant false alarm rate
DSP	digital signal processing
D/A	digital-to-analog
DS	direct sequence
DS-CDMA	direct sequence code division multiple access
DOV	direction of arrival
E-CFAR	excision CFAR
FDMA	frequency division multiple access
FH	frequency hopping
FH-CDMA	frequency hopping code division multiple access
FPC	full period code
GCMLD	generalized censored mean level detector

GTL-CMLD	generalized two-level censored mean level detector
GO-CFAR	greatest of CFAR
IS-95	Interim Standard 95
ISI	inter-symbol interference
LMS	least mean square
ML	maximum likelihood
MLAP	mean level acquisition processor
MSE	mean square error
MV	minimum variance
MAI	multiple access interference
NLOS	non-line-of-sight
OSAP	order statistics acquisition processor
OS-CFAR	order statistics CFAR
PPC	partial period code
PSK	phase shift keying
PN	pseudo-noise
QPSK	quadrature PSK
RF	radio frequency
SOI	signal of interest
SNOI	signals not of interest
SINR	signal-to-interference plus- noise ratio
SIR	signal-to-interference ratio
SNR	signal-to-noise ratio
SO-CFAR	Smallest of CFAR

S-CFAR	switching CFAR
SOS-CFAR	switching ordered statistic CFAR
TDMA	time division multiple access
TM-CFAR	trimmed mean CFAR
ULA	uniform linear array
UMTS	Universal Mobile Telecommunications System
VI-CFAR	variable index CFAR

Chapter 1

General Introduction

Summary

In this chapter, we present an introduction to the research topic and the specific problem under consideration. Then we give a literature review presenting some of the related research work in this rich literature. We give an explanation and the purpose of this thesis and the research objectives. Then, the chapter is concluded with a section presenting the organization of the thesis.

1.1 Introduction

1.2 Literature Review

1.3 Objectives

1.4 Organization of the Thesis

1.1 Introduction

For years, direct sequence code division multiple access (DS-CDMA) appears as one of the most favored technique for cellular communication systems. The Interim Standard 95 (IS-95) from the second generation cellular standards, and the cdma2000 and the Universal Mobile Telecommunications System (UMTS) from the third generation cellular standards all are some examples of the DS-CDMA technique. The amount of interest and effort invested in this area by research institutions and industry is gigantic and constantly growing. DS-CDMA communication systems have received considerable interest in the literature and the problem of pseudo-noise (PN) code acquisition is one of the topics that have been studied extensively.

To transmit a data signal in the direct sequence (DS) communication systems, the sender uses a PN code to spread the signal before transmission. This same code is then used by the receiver for the despreading operation. To be able to demodulate properly the received signal, the receiver must first perform the PN codes synchronization between the received code and the locally generated one. The goal of this process is to align these two PN code sequences, which is achieved in two stages; (1) PN acquisition, which coarsely aligns the two PN code sequences within a fraction of the chip duration, and (2) PN tracking, which is a finer alignment that aims to reducing synchronization errors to an acceptable limit [2].

Due to the unknown time delay between the transmitter and the receiver, the phase of the received PN code is unknown. Therefore, all possible phases of the spreading PN code will form an uncertainty region of phases that can be divided into a number of cells; each cell corresponds to a different phase delay. To find the correct code phase, the receiver in the PN code acquisition stage searches over these cells.

According to the search mechanism, the acquisition stage can be classified as: the serial search acquisition in which one uncertainty code phase is tested at a time [3-4], the parallel search acquisition in which all possible code phases are tested simultaneously [5-6], and the hybrid search acquisition which combine the serial search with the parallel search [2,7]. To determine whether the tested phase cell is a synchronized code phase, that is the local code and the received PN code sequence are aligned or not, the correlation between these two PN codes is computed and compared to a threshold value to make the synchronization decision.

The PN code acquisition can be modeled as a binary hypothesis problem, where the code phase cells represent either H_1 hypothesis for the correct phase that results in the synchronization (the alignment) state or H_0 hypothesis for the incorrect code phase that results in the non-synchronization (the non-alignment) state. The receiver seeks to make a correct decision by accepting H_1 code phases and rejecting H_0 code phases and trying to avoid as much as possible the miss and the false alarm situations [8].

PN acquisition is the most challenging stage in code synchronization. In mobile communications it is known that the receiver receives multiple copies of the transmitted signal from several paths with different attenuations and time delays, furthermore the multiple access interference (MAI) signals are common in DS-CDMA communication systems. In addition to that, the power of the received signal is inversely proportional to some power n of the distance between the transmitter and the receiver, where n is normally between 3 and 4 [9]. All these circumstances have serious effects on the PN code acquisition performance. Moreover, since the received signal levels are unknown and location varying, using a fixed threshold may cause too many false alarms and/or low detection probability according to the selected threshold value [8-9]. If the

threshold value is too low, the false alarm probability will increase seriously. On the other hand, if it is too high the probability of miss is increased [8].

An efficient PN code acquisition is a significant requirement for DS-CDMA wideband communication receivers. It is essential to acquire the PN code sequence both quickly and accurately in order to provide a high quality communication.

1.2 Literature Review

To overcome the excessive false alarms that may result from using the fixed threshold, a threshold value set adaptively according to the surrounding environment to maintain a constant false alarm rate (CFAR) has been proven to give best results. CFAR algorithms are well developed in the field of automatic radar signal detection. The main idea is to estimate the background noise variance or power, which is not known, from a reference window consisting of a number of cells to set the threshold adaptively [8].

Finn and Johnson [10] proposed the cell-averaging constant false alarm rate (CA-CFAR) detector. The adaptive threshold is obtained from the maximum likelihood estimated noise power, which is the arithmetic mean of the output of the reference cells. In a homogeneous environment, the samples in the reference cells are assumed to be independent and identically distributed (i.i.d.). In this case, the probability of detection of the CA-CFAR detector approaches the probability of detection of the optimum Neyman-Pearson detector as the number of reference cells becomes very large. Under non-homogeneous conditions and in multiple interference situations, the performance of the CA-CFAR detector deteriorates seriously and many detectors have been proposed in the literature to improve the detection performance [11-24]. In [11], Rohling proposed the order statistics CFAR (OS-CFAR) detector in which one cell is chosen to represent the estimate of the noise power after rank ordering the contents of the cells in the

reference window. Cho and Barkat [12] proposed the moving OS-CFAR detector for non-homogeneous situations. Rickard and Dillard [13] proposed the censored mean level detector (CMLD) in which the reference cells are rank ordered and the highest cells containing interferences are censored. The performance of the CMLD for a known number of interferences has been studied in [14]. Gandhi and Kassam [15] proposed the trimmed mean CFAR (TM-CFAR) detector. In the TM-CFAR detector, the noise power estimation is the mean of the rank ordered reference cells after censoring a number of cells from the both ends (lower end and upper end) of the reference window. When the number of interferences is not known *a priori*, Barkat et al. [16] proposed the generalized censored mean level detector (GCMLD), in which cells containing interferences are determined and censored. When the background noise level presents a transition of two levels in addition to interferences, Himonas and Barkat [17] proposed the first concept on automatic censoring in CFAR processing and called the detector the generalized two-level censored mean level detector (GTL-CMLD), which censors automatically unwanted interferences. In [18], Smith and Varshney introduced the variable index CFAR (VI-CFAR), an intelligent CFAR processor based on data variability. Automatic censoring based on ordered data variability in a multi-interference environment was also considered in [19]. In [20], Cao proposed the switching CFAR (S-CFAR) in which the magnitude of the test cell is exploited to select appropriate reference cells for the noise power estimation. Meng [21] comments on the S-CFAR by proposing a simpler approach based on order statistic to obtain alternative expressions for the probabilities of false alarm and detection, and in a paper to appear in January 2013, Zhang et al. [22] proposed an improved switching CFAR detector for non-homogeneous environments. Erfanian and Vakili [23] proposed a switching ordered statistic CFAR (SOS-CFAR) for different radar environments. A MATLAB

simulation study of some CFAR implementation cost and performance tradeoffs in heterogeneous environments was considered in [24].

CFAR processing has found a fertile environment in adaptive PN code acquisition for wideband DS-CDMA communication systems. Several researches have been proposed in literature which employing the CFAR processing to set an adaptive threshold for the PN acquisition [9, 25-28]. In [25], Benkrinah and Barkat considered an adaptive PN code sequence acquisition using the OS-CFAR in DS-CDMA communication systems for a multipath Rayleigh fading channel. In [26], the channel was assumed to be a non-fading additive white Gaussian noise (AWGN) and the CA-CFAR processing was used to compute the adaptive threshold. The simulation results have shown that this system gave a better performance than the conventional system with a fixed threshold.

Kim et *al.* considered in [9] two adaptive acquisition schemes for PN code sequences; CA-CFAR processing which they called mean level acquisition processor (MLAP) and OS-CFAR which they called order statistics acquisition processor (OSAP) in Rayleigh fading. However for the OS-CFAR they select the smallest ranked cell which may result in higher false alarm rates. In [27] the CMLD was renamed as adaptive acquisition processor (AAP) and considered multipath fading channels. The excision CFAR (E-CFAR) was considered in [28] for adaptive PN acquisition in DS spread spectrum communication. The idea of excision CFAR was actually first introduced in 1988 by Barkat [29] and called it a modified CFAR detector.

Today many DS-CDMA communication systems rely on multiple antennas for both reception and/or transmission. Using multiple antennas to improve PN acquisition performance has received considerable interest in the literature. Two different

approaches for the multiple antennas can be considered depending on the inter-element separation and the signal processing on the reception of the signals. Multiple antennas either are in the form antenna diversity or in the form of smart antenna (adaptive antenna array with beamforming) [30]. Antenna diversity uses enough distance between antenna elements to ensure that the corresponding channels have independent fading processes. In practice this separation depends on the angular spread characterization of the radio channel. Narrow angular spreads require considerable antenna separation, whereas closer separation is sufficient in large angular spreads to obtain independent channel behavior. An improvement in the signal-to-noise ratio (SNR) will result from the noncoherent combining of received signals from each antenna, which in turn, improves the statistics of the detector, and consequently the acquisition [30].

PN code synchronization utilizing antenna diversity has been widely discussed in the literature. In [6] Rick and Milstein have investigated the use of antenna diversity to improve the conventional parallel acquisition performance of a DS spread spectrum signal in both Rayleigh and Rician amplitude distributions. In [31], Krouma and Barkat considered a hybrid double-dwell system with antenna diversity for DS-CDMA using the CA-CFAR processing in Rayleigh fading channels. An extended version was considering computations of the time acquisition and more comparison with a hybrid single dwell was given in [32]. In [33], Kwon *et al.* considered the three fundamental CFAR processors; CA-CFAR, greatest of CFAR (GO-CFAR) and the smallest of CFAR (SO-CFAR) in a hybrid PN acquisition of DS-CDMA communication systems for both homogenous and non-homogeneous environment. In [34], Bekhakhecha *et al.* considered an adaptive PN code acquisition using antenna diversity and OS-CFAR processing. They evaluated the detection performance of the proposed scheme in a

frequency selective fading channel and the simulation results showed a substantial performance improvement.

Due to many distinctive advantages of using smart antenna, there was a focus on utilizing a smart antenna to improve PN acquisition in the last few years [1, 35-37]. Smart antenna has a good ability in combating MAI signals, tracking mobile signals, reducing multipath fading, and improving signal power gain [1]. Wang and Kwon [35] proposed an efficient PN code acquisition scheme that used all smart antenna elements during PN code acquisition. The results showed that employing all antenna elements for PN acquisition has improved the detection performance and the mean acquisition time compared to using just a single antenna for the acquisition under AWGN and Rayleigh fading channels. In [36], the same authors try to make an iterative estimation of the received power using the iterative weights obtained from the least mean square (LMS) algorithm to compute iteratively a new threshold for a better PN code acquisition for each cell. This requires extremely heavy computations and the assumption that the smart antenna can track the direction of arrival (DOA) estimation of the desired user signal perfectly, and yet it does not yield a constant false alarm rate. The DOA with beamforming with a fixed threshold for PN acquisition was considered by Puska *et al.* in [37].

In new recent research, Sofwan and Barkat [1] provide a novel approach for PN code acquisition using smart antenna and adaptive thresholding TM-CFAR processing to achieve the design probability of false alarm rate (CFAR). In addition, the results have shown a serious enhancement of the detection probability in a Rayleigh slowly fading multipath channel compared to the scheme in [35].

1.3 Objectives

It has been shown that the communication system proposed by Sofwan and Barkat [1] using smart antennas and adaptive thresholding CA-CFAR processing has comparable detection performance as the smart antennas system proposed by Wang and Kwon [35] in a homogeneous environment. In a non-homogeneous environment, in the presence of multipath and MAI signals, the detection performance of both systems in [35] and in [1] with CA-CFAR processing is seriously degraded. To remedy to this situation, the trimmed mean (TM) CFAR was detector was suggested in [1], and consequently the system performance improved substantially and thus showed robustness in a more realistic. In today's mobile communication, the environment is non-homogeneous with the presence of both multipath and MAI signals.

The robustness of the communication system proposed in [1] suggests the consideration of even other robust CFAR processors based on order statistics.

In this thesis, we consider the system proposed in [1] while using the CMLD-CFAR as an adaptive threshold in a Rayleigh slowly fading multipath communication channel. The CMLD-CFAR is one of the order statistics CFAR processors that has proved to be robust in non-homogeneous environments with multiple interfering signals [13-14]. As mentioned earlier, in the TM-CFAR the ordered cells of reference window are trimmed or censored from both the upper and the lower end, while in the CMLD-CFAR the ordered cells are censored only from the upper end. So the CMLD-CFAR can be considered as a special case from the TM-CFAR.

In the system, the transmitted signals are received by all elements of the smart antenna and go through the LMS adaptive processor. Then, the output from the LMS processor undergoes CMLD-CFAR processing in order to make a cell synchronization

decision. In the CMLD-CFAR, the outputs from the reference cells are rank-ordered according to their magnitude and the highest cells which correspond to multipath replicas and multiple access interferences are censored to avoid unnecessary high thresholds, while the other remaining cells are used to compute the estimate of the background power level which will be used as the adaptive threshold. This will be explained in more detail in the next chapter.

In [1], expressions for the conditional probability density functions of the aligned and the non-aligned hypotheses at the output of the LMS were developed. Based on these expressions, the probability of false alarm of the proposed system that consider the TM-CFAR was derived and the detection performance has been simulated to show the robustness of the system in combating MAI and multipath signals in non-homogeneous environment. In this thesis, we will use those probability density functions of the LMS output in deriving closed form expressions for the probability of false alarm, the probability of detection, and the mean acquisition time for the proposed system. Then we study how efficient is the proposed system in a Rayleigh slowly fading multipath channel. The effect of employing all elements of the smart antenna on the PN acquisition performance compared to the AAP processor considered in [27] will also be investigated. The detection and the mean acquisition time performances will also be studied in terms of computer simulations under various design parameters.

And we would like to point out that, part of this research work (the derivation of the probability of false alarm and some obtained results for the detection performance) has been published as a research paper [38] in *IEEE International Conference on High Performance Computing and Communications* (IEEE-HPCC 2012), Liverpool, UK, June 2012.

1.4 Organization of the Thesis

The rest of the thesis is organized as follows. Chapter 2 provides the necessary preliminaries of spread spectrum communication, code division multiple access (CDMA), PN code acquisition for direct sequence receiver, adaptive thresholding CFAR processing, and smart antenna.

In Chapter 3, we present the communication system under consideration for wireless wideband communication. We present a detailed analysis of the proposed system while we derive closed form expressions for the probability of false alarm, the probability of detection, and the mean acquisition time. An in-depth analysis of the MATLAB simulations results on the performance of the system is presented along with our conclusions.

In Chapter 4, we present a summary of the work done in this thesis plus some suggestions for future research work.

Chapter 2

Spread Spectrum Communication, Adaptive Thresholding CFAR Detection, and Smart Antenna

Summary

In this chapter, we present the necessary theoretical background information for the research topic under consideration. The major topics needed are spread spectrum communications, adaptive thresholding CFAR detection and smart antenna. Hence, we first give an overview on spread spectrum communication and code division multiple access (CDMA). Then, PN code acquisition in direct sequence CDMA receivers is discussed. The concepts of signal detection and adaptive thresholding constant false alarm rate (CFAR) processing are then presented. We conclude the chapter with a section on smart antennas.

2.1 Introduction

2.2 Spread Spectrum

2.3 Code Division Multiple Access

2.4 PN Code Acquisitions for Direct Sequence Receiver

2.5 Adaptive Thresholding CFAR Detection

2.6 Smart Antenna System

2.1 Introduction

Wireless communication systems are one of the fast growing technologies and are becoming increasingly important in many fields of our daily life. Wireless communications rely on multiple access techniques to share the limited frequency spectrum between users. Multiple access communications determine the way signals of multiple senders share the spectrum with no or low interference, so the receivers are able to distinguish the senders' signals. The most common used multiple access techniques are: frequency division multiple access (FDMA), time division multiple access (TDMA), and code division multiple access (CDMA).

In FDMA, the available frequency spectrum is divided into several disjoint frequency bands which are assigned to each individual user as shown in Fig. 2-1(a). So, all users can transmit simultaneously (i.e., at the same time) using these small bandwidth channels. On the other hand, TDMA divides the transmission time into a series of repeating fixed time intervals called frames which are composed of a number of time slots as shown in Fig. 2-1(b). Each slot is assigned to one user, so he/she is allowed to either transmit or receive in this time period of the frame. The users transmit sequentially using all the available bandwidth. In FDMA/TDMA, each user is supplied with certain resource, frequency/time slot, which is disjoint from those of any other user. A completely different approach is CDMA which does not require allocation of disjoint frequency or time resources to each user. Instead the system allocates all resources to all users as shown in Fig. 2-1(c). Unique channels are created by assigning each user a unique code sequence that is uncorrelated with other users' codes. [39-40]

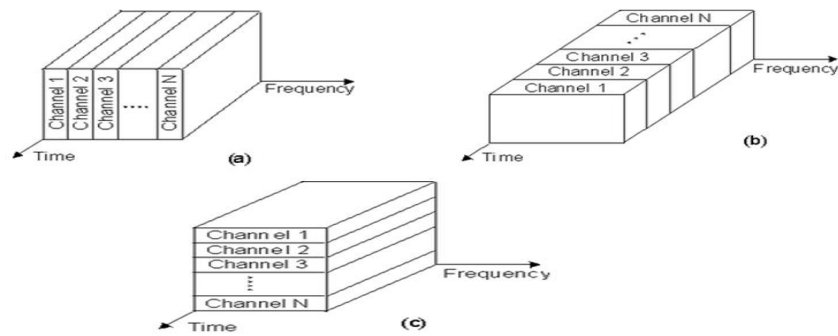


Fig. 2-1: The multiple access techniques: (a) FDMA, (b) TDMA, and (c) CDMA.

CDMA is the most popular modulation technique in spread spectrum wireless communications.

2.2 Spread Spectrum

Over the years, with the development of mobile phones, spread spectrum communication has become more and more popular. Spread spectrum systems have been developed in the mid-1950's for military communications. The primary purposes of these systems were to:

- Hide the presence of the signal,
- Protect the signal from eavesdropping, and
- Provide a high resistance against strong intentional interferences (jamming).

Later it was realized that this technique provides powerful advantages, such as:

- Anti-interference,
- Multiple users access communications,
- High resolution ranging, and
- Accurate universal timing.

This benefits other civilian communication systems such the cellular mobile communications, timing and positioning systems, and some specialized applications in satellites. [39-40]

2.2.1 What is the Spread Spectrum?

In [40] spread spectrum communication is defined as: “Spread spectrum is a means of transmission in which the signal occupies a bandwidth in excess of the minimum necessary to send the information; the band spread is accomplished by means of a code which is independent of the data, and a synchronized reception with the code at the receiver is used for despreading and subsequent data recovery”. From this definition we see that the spreading operation over a large bandwidth is done by using an independent code sequence (called PN code sequence). The resulting wideband signal will be hard to jam since it occupies a large band of frequencies embedded in noise as compared to narrowband signals; in addition it will be hard to detect its presence. To despread the received signal, the receiver needs to use a synchronized version of the PN code sequence. Fig. 2-2 shows a block diagram of the spread spectrum communication system. [41-42]

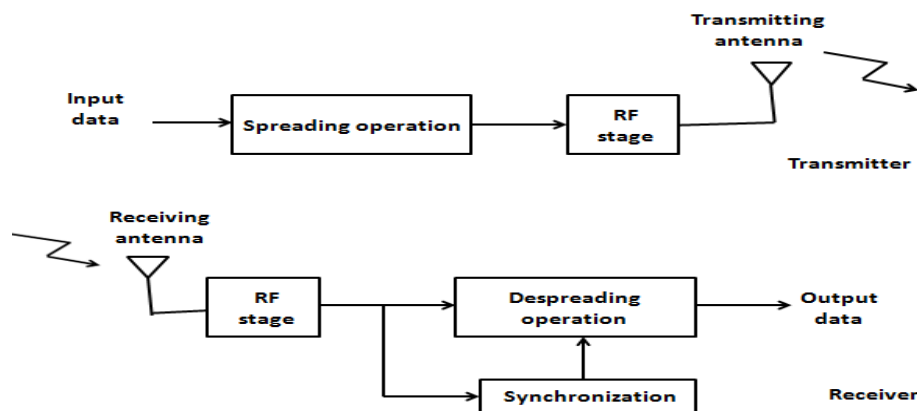


Fig. 2-2: Spread spectrum system.

2.2.2 Pseudo Noise Code Sequences

The PN code sequence or sometimes called pseudo random sequence is a noise-like (but deterministic) signal that is used for bandwidth spreading. It is a sequence of 1's and 0's called chips with a chip rate higher than the data signal's bit rate. This code sequence is generated satisfying the following properties [42-43]:

- (i) It is a periodic signal known to the transmitter and the receiver.
- (ii) Its autocorrelation function has properties similar to the white noise signal, it has sharp autocorrelation peak (for that it is named pseudo noise). This property will help in the synchronization process.
- (iii) It should be balanced, that is the difference between the number of 1's and 0's in each period should be at most one. With poor balance property, spikes will be seen in the spectrum so the signal will be easily detectable.

Using this code sequence for spreading, the baseband narrowband signal becomes wideband and appears noise-like. There are many types of the PN code sequence, for example: m-sequence code, Gold code, and Hadamard-Walsh code. But it is important to select the appropriate code because the type and length of the PN code sequence set the bounds on the communication system capability [43].

2.2.3 Types of Spread Spectrum

Many spread spectrum technologies are currently available, the direct sequence (DS) spread spectrum and the frequency hopping (FH) spread spectrum are the most commonly used spread spectrum techniques. Both generate wideband signals controlled by the PN code sequences. But they differ in the way of employing those codes in the

spreading operation and how the resulted spreading signals occupy the large frequency band. In the following, a description of those types of spread spectrum is given.

Direct Sequence Spread Spectrum

DS spread spectrum communication is the most used modulation technique due its ease of implementation. The narrowband data signal is spread by multiplying it directly with the PN code sequence and transmitted after being modulated. Since the chip rate is higher than the data bit rate, the signal will gain a large bandwidth as shown in Fig. 2-3. If the total signal power is interpreted as the area under the spectral density curve, we observe that spreading the narrowband signal over a wide bandwidth the signal's power level (the power spectral density) is reduced and becomes embedded in noise [41- 42].

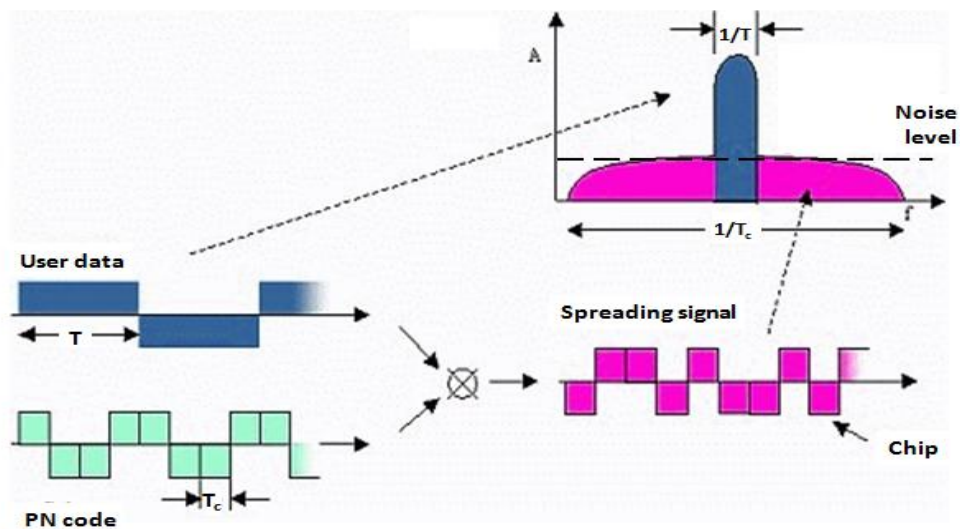


Fig. 2-3: Direct sequence spreading operation.

The transmitted DS spreading signal occupies the entire large frequency band continuously and its carrier stays at a fixed frequency. At the receiver, the local PN code sequence is multiplied with the received wideband signal to despread the received signal and obtain the original narrowband signal. On the other hand, if for example there

is an interfering jamming signal, the multiplication with the PN code will spread it. Consequently, the impact the jammer is greatly reduced as shown in Fig. 2-4. This is one of the main reasons spread spectrum communication is less vulnerable to interferences [42].

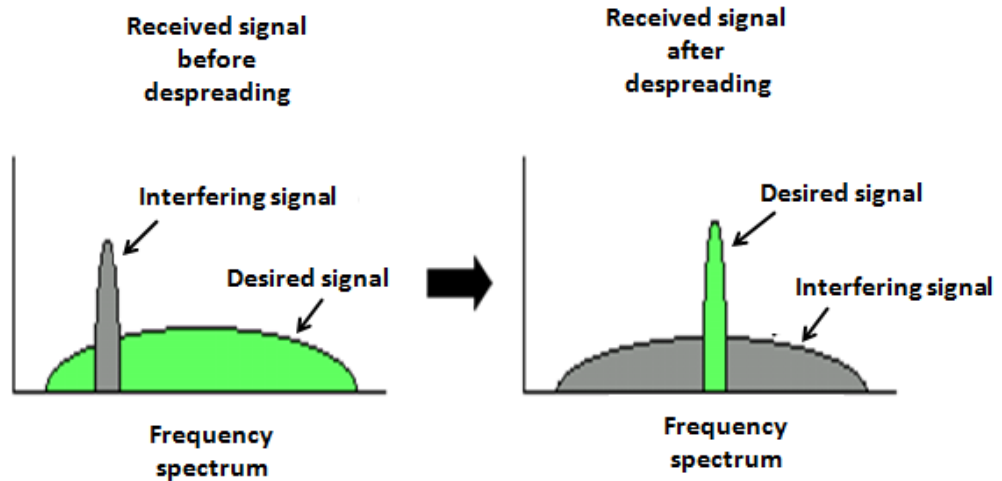


Fig. 2-4: Direct sequence despreading operation [website].

Frequency Hopping Spread Spectrum

In FH spread spectrum, the spreading over a wide bandwidth is not achieved by widening the total signal power of the narrowband signal as in direct sequence, but it is achieved instead by hopping from frequency to another frequency at regular time intervals within the large frequency band as shown in Fig. 2-5. The PN code sequence, in this case, is used to shift the carrier frequency of the narrowband signal in a pseudo random manner [42]. At the receiver, the synchronized PN code sequence is used to determine the different carrier frequencies at the different time intervals. The FH spread spectrum avoids the location of a jamming signal by hopping in short times between a large set of frequencies. FH does not have the same degree of jamming resistance as DS spread spectrum. When there is a jamming signal in a frequency to which the signal will hop to it, a collision will occur and the data will be lost [41].

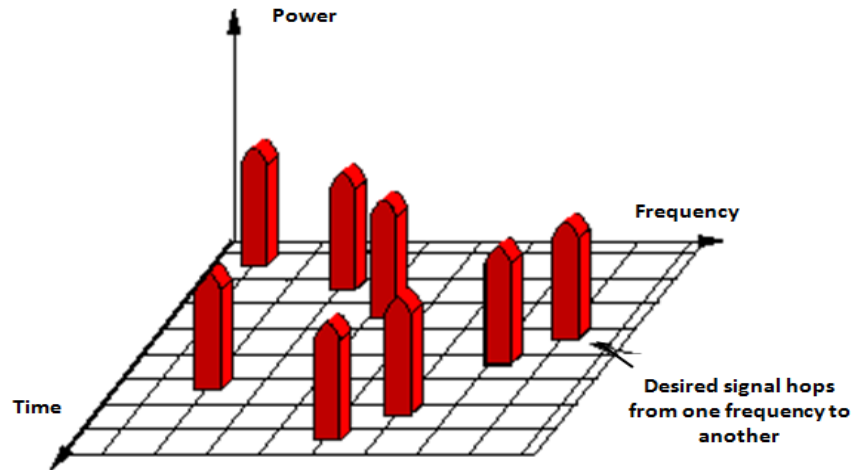


Fig. 2-5: Frequency hopping spread spectrum [website].

2.3 Code Division Multiple Access

In direct sequence code division multiple access (DS-CDMA) each user will spread his signal by using a different PN code which is (approximately) orthogonal to the PN codes of all other users. Therefore, the receiver needs to perform a correlation operation to detect the signal addressed to a given user. The other users' signals will appear as noise due to the low cross-correlation property as shown in Fig. 2-6.

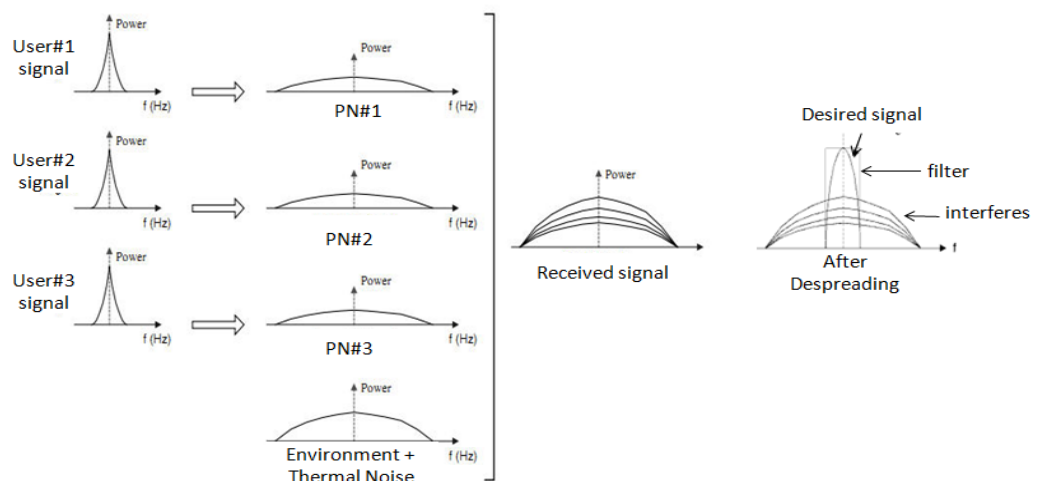


Fig. 2-6: DS-CDMA.

In frequency hopping code division multiple access (FH-CDMA), each user will select one of available frequencies within the wide band channel as a carrier frequency. The pseudorandom changes of the carrier frequencies randomize the occupancy of a specific band at any given time, thereby allowing for multiple access over a wide range of frequencies [39].

The focus will be on DS-CDMA, which is the communication scheme considered in this thesis, and also it is the most popular scheme in spread spectrum communication.

DS-CDMA Transmitter

A functional block diagram of the DS-CDMA transmitter is shown in Fig. 2.7

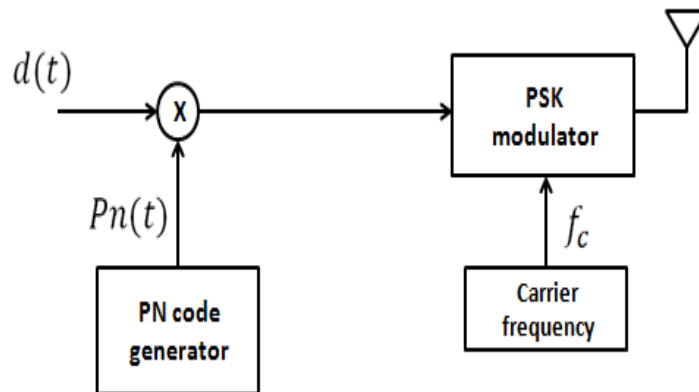


Fig. 2-7: DS-CDMA transmitter.

The transmitted signal $d(t)$ with a data bit rate $R_d (= 1/T)$ is first multiplied with the sender's PN code sequence $Pn(t)$ that has a chip rate $R_c (= 1/T_c)$ which is an integer multiple of R_d . The effect of multiplication is to spread the baseband bandwidth $BW_d \cong R_d$ of $d(t)$ over a large bandwidth $BW_{ss} \cong R_c$. After the spreading process, a PSK (phase shift keying) modulation is performed on the resulted baseband signal to transmit a bandpass signal with a pseudorandom phase shift. BPSK (binary PSK) and

the QPSK (quadrature PSK) are commonly used for PSK modulation in practical systems [43].

DS-CDMA Receiver

To retrieve the data signal $d(t)$, the receiver will perform despreading and demodulation operations on the received spreading signal. These operations require a synchronized local PN code sequence $P_n(t)$ (for the despreading operation) and a synchronized carrier (for the PSK demodulation operation). Therefore, a synchronization process must be done before and during these two operations.

The need synchronization process is a result of an initial timing and frequency uncertainty between the transmitter and the receiver for the following reasons [8]:

1. Uncertainty in the range between the transmitter and the receiver, which translates into uncertainty in the amount of propagation delay.
2. Relative clock instabilities between the transmitter and the receiver, which results in phase differences between the transmitter and the receiver spreading signals.
3. Uncertainty of the receiver's relative velocity with respect to the transmitter, which translates into uncertainty in a Doppler frequency offset value of the incoming signal.
4. Relative oscillator instabilities between the transmitter and the receiver, which results in frequency offset between the incoming PN sequence and the locally generated sequence.

There are two models for DS-CDMA receivers according to the placement of the PSK demodulation relative to the despreading process. In the *non-coherent* receiver, the

despreading of the received signal is performed prior to the PSK demodulation as shown in Fig. 2-8.

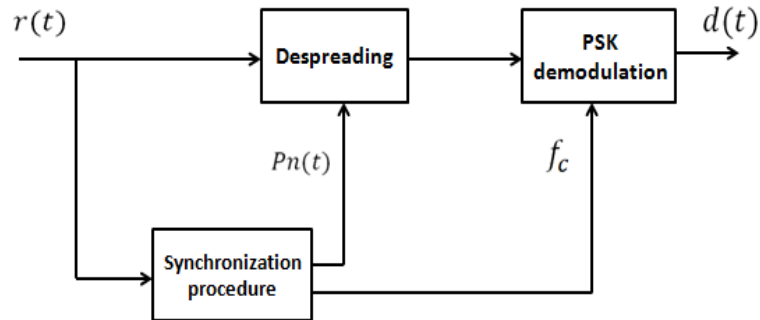


Fig. 2-8: Non-coherent DS-CDMA receiver.

When the despreading process is performed after the PSK demodulation as shown in Fig. 2-9, the receiver is called a *coherent* (or synchronous) receiver.

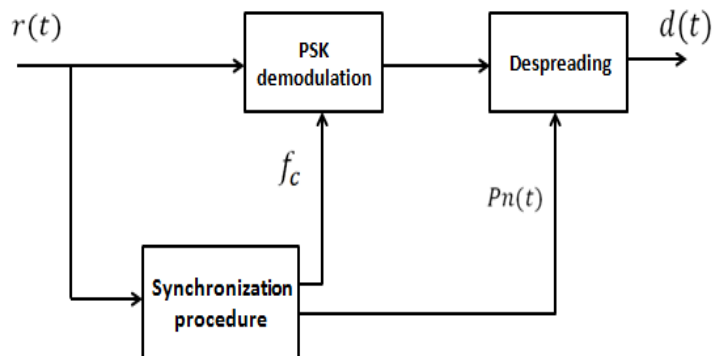


Fig. 2-9: Coherent DS-CDMA receiver.

2.4 PN Code Acquisition for Direct Sequence Receiver

In spread spectrum communications, the locally generated PN code sequence at receiver must be synchronized with the received PN code sequence to be able to despread the received signal and detect it. Synchronization must be within a small fraction of chip duration. Otherwise, due to the orthogonality principle, insufficient signal energy will

reach the receiver data demodulator. Typically, the process of synchronization is performed in two stages: first, the PN code acquisition stage, and then the PN code tracking stage. The PN code acquisition is a process of bringing the two PN codes into coarse time alignment to within a fraction of the chip duration. Once the acquisition process is achieved, the PN code tracking process is initiated which aims to reducing the synchronization errors to an acceptable limit for maintaining the two PN codes in fine synchronism [39, 44].

The PN code acquisition process may be viewed as an attempt to synchronize the receiver clock to the transmitter clock. Even though extremely accurate clocks are used in spread spectrum communication systems to reduce the time uncertainty between the receiver clock and the transmitter clock, the propagation delay in the transmitted signal through the channel and the propagation effects such as multipath produce uncertainty at the receiver about the timing (phase) of the received PN code sequence. This time uncertainty region which is a region of all possible phases of the received PN code sequence is typically divided into a finite number of cells, where each cell corresponds to a different phase delay and the receiver must determine which one of the cells is the phase of the received PN code sequence. So in the initial synchronization (acquisition) stage, the receiver searches through those potential code phases, each phase is evaluated or tested by attempting to despread the received signal. If this tested code phase is correct (i.e. synchronized code phase), despreading of the received signal will occur and thus it will be detected. Otherwise, in case of incorrect phase, the received signal will not be despread [39].

The acquisition process can be modeled as a binary hypothesis problem. When synchronization is achieved we have hypothesis H_1 ; otherwise, we have the null

hypothesis H_0 in the tested code phase. For the tested code phase in the PN code acquisition process, the receiver must make a decision based on some criterion in favor of hypothesis H_1 or hypothesis H_0 . Detection consists of deciding in favor of the H_1 hypothesis when the tested code phase is truly the synchronized code phase. Also, deciding in favor of H_0 hypothesis when the tested code phase is truly in non-synchronization situation is a correct rejection. When the receiver makes a decision in favor of hypothesis H_1 , while actually H_0 is true, it is called a *false alarm*. Deciding in favor of hypothesis H_0 when H_1 is true is called *miss*. The probability of the first wrong decision called the probability of false alarm (P_{fa}) while the probability of the second wrong decision called the probability of miss (P_M). This terminology is borrowed from the radar nomenclature [8].

There are several search strategies that can be selected to scan the cells (code phases) in the uncertainty region for PN code acquisition. The received and local PN code signals are first multiplied to produce a measure of the correlation between these two codes. This measure can be obtained by using an active correlator or a passive matched filter. In the active correlator, the received PN code signal is multiplied with a continuously running local generated PN code signal and then integrated over a time interval often called the dwell time to get the correlation measure. In the passive matched filter, the received PN code signal is convolved with a fixed local PN code signal. In this configuration, the input continuously slides past the stationary (not running in time) local PN code until the two are in synchronism. The obtained correlation measure is then passed to a suitable detector/decision rule to decide whether the two codes are synchronized or not for the tested code phase. The differences between the various PN code acquisition schemes depend on the type of detector (decision strategy) used, and the adopted search strategy which acts on the detector

outputs to make the final decision. Consequently, PN code acquisition schemes can be classified in different ways based on the detectors and the search strategies. The most commonly used detector for acquisition in DS-CDMA communication receivers is the noncoherent detector in which the despreading operation is performed before the carrier phase synchronization [44].

The time it takes to test a cell for synchronization is called the *dwell time* and is approximately equal to the length of the integration time interval in the active correlator. PN acquisition is achieved by *single dwell* or *multiple dwell* detectors. This classification is based on whether the acceptance of the tested code phase cell as a synchronized code phase can be made based on a single test (single dwell) or verification tests must occur before a decision about synchronization is made (multiple dwell). Depending upon the duration of the dwell time interval relative to the PN code period, the single dwell time detector can be further classified according to whether they utilize partial period code (PPC) or full period code (FPC) correlation. In multiple dwell detectors, the detection of a synchronized code phase cell in the first test (searching mode) must be followed by multiple tests (verification mode) to make the final decision about synchronization. The dwell time of the first test is usually much shorter than the dwell times of verification tests in order to avoid spending a long time on the rejection of non-synchronized code phase cells. The multiple dwell detectors differ from one another in the strategies for verification. The verification mode can employ *immediate-rejection* logic or *non-immediate-rejection* logic. In the immediate-rejection case, the tested cell is immediately rejected as a non-synchronized code phase cell as soon as a single test in the verification mode tests is failed. The non-immediate-rejection case uses a majority logic type of decision on the total set of verification mode tests [3, 44-45].

The adopted criterion for testing cells for synchronization decision can be a factor that distinguishes one detector from another. Classical approaches using fixed thresholds may be Bayes criterion, Neyman-Pearson criterion, or some other criterion [8, 44] which are sensitive to noise power changes and to the number of interferences and multipath leading to excessive false alarm rates. A suboptimum approach using adaptive thresholding based on constant false alarm rate (CFAR) computes an adaptive threshold based on the maximum likelihood estimation of the noise power in the test cell obtained from the neighboring cells in the reference window while maintaining the probability of false alarm constant [8]. The concepts of adaptive thresholding CFAR detection will be explained in the next section.

A summary of the above classification for the different types of PN code acquisition schemes based on the used detectors is illustrated in Figure 2-10.

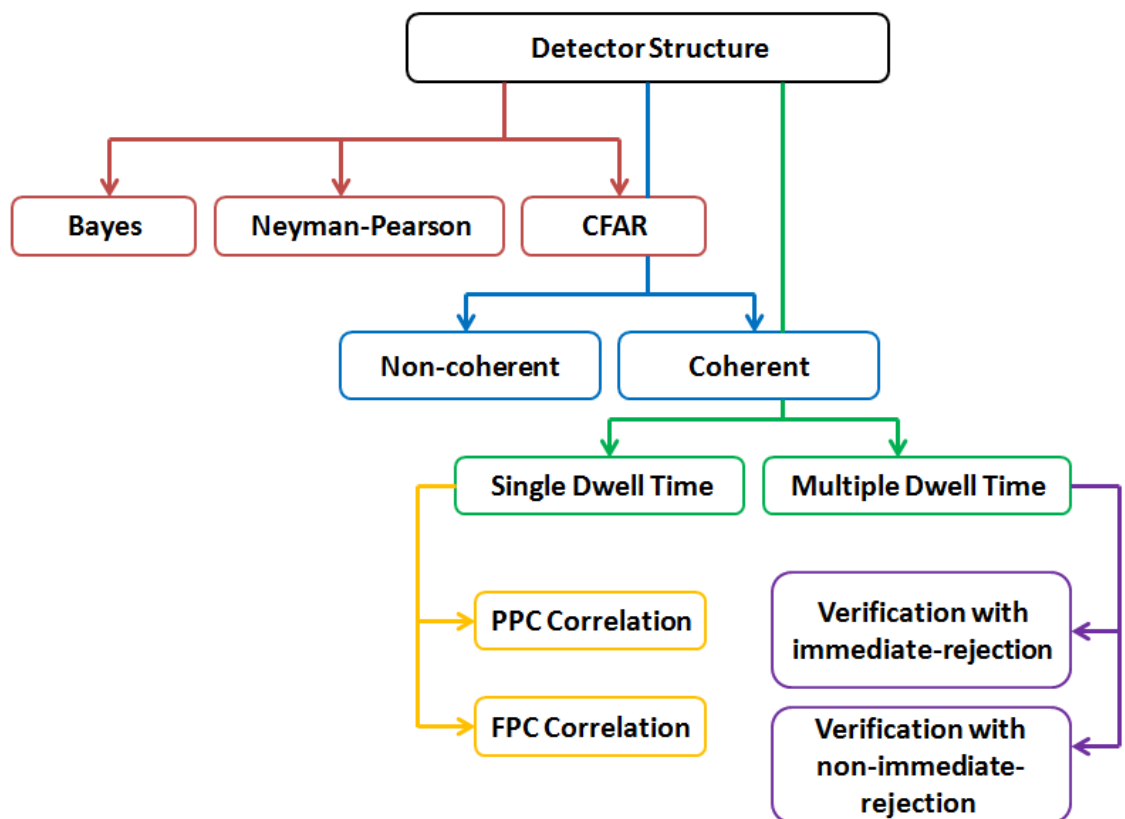


Fig. 2-10: A classification of the PN code acquisition schemes based on the detector structure.

The PN code acquisition searching procedure can be classified into three methods; namely, the *serial* search methods, the *parallel* search methods, and the *hybrid* search methods. The serial search means stepping through the uncertainty region serially; one uncertainty phase is tested at a time. The advantage of this search method is the hardware simplicity, but in the case of a long PN sequence it has a long acquisition time. In contrast, the parallel search method tests all the uncertainty phases simultaneously. This search method has a fast acquisition time, but for a long PN sequence the hardware complexity increases dramatically and that is why it is impractical. As a trade-off between the acquisition time and the hardware complexity, the hybrid search scheme has been proposed which combines the parallel search with the serial search in order to cover the whole uncertainty region [2, 7].

2.5 Adaptive Thresholding CFAR Detection

PN code acquisition with a fixed threshold value is unable to adapt to the varying mobile communications environment and may result in a high false alarm rate and/or low detection probability. Thus, adaptive thresholding CFAR detection has proved its robustness in mobile communications environments. The concepts of CFAR processing are well developed in the field of radar signal detection.

2.5.1 Adaptive CFAR Detection

One of the main goals in radar signal detection systems is to detect the presence of a target within the area of observation. The received signal is compared to a threshold value and a target is declared present whenever the signal exceeds the threshold. The optimal Neyman-Pearson detector requires a complete statistical description of the received signals and noise. This information may not be available *a priori* and the statistics of the received signal may not be stationary (varying with time) [8].

In real radar applications, the problem is to detect targets embedded in noise and clutter. Clutter is a term applied to any undesired signal to the radar user. The received signal is usually statistically nonstationary with an unknown variance due changes in the environment. Consequently, using the optimal Neyman-Pearson detector with a fixed threshold is no longer valid because it is an extremely sensitive to the total noise (thermal noise plus clutter) variance. In fact, a small increase in the total noise power from the design value results in a corresponding increase of several orders of magnitude in the probability of false alarm. This is illustrated in Fig. 2-11, for a design probability of false alarm of 10^{-6} , an increase of only 3 dB in the noise power causes the actual probability of false alarm to increase by more than 1000, which is intolerable for data processing, either by a computer or by a human operator. Thus, adaptive thresholding processing is needed to maintain a constant false alarm rate (CFAR) [8].

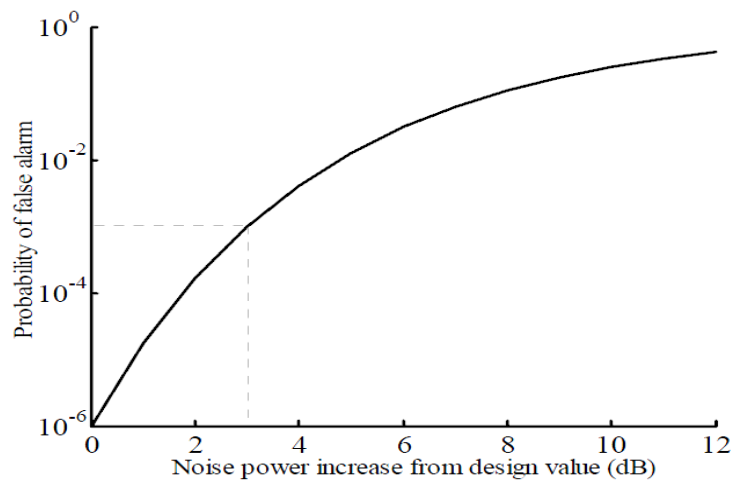


Fig. 2-11: Effect of the noise power increase on the probability of false alarm for a fixed threshold [8].

Finn and Johnson [10] proposed the cell averaging CFAR (CA-CFAR) detector in which an estimate of the noise environment is obtained from the arithmetic mean of the

output of the reference cells. The reference window consists of N_c reference cells surrounding the cell under test (CUT), which is generally assumed to be the cell in the middle of the reference cells. Some adjacent cells to the CUT, called *guard cells*, are ignored from the noise estimate in order to avoid any signal energy spill from the CUT into these adjacent cells which may affect the total noise power estimation. $N_c/2$ cells form a *lagging window* and the other $N_c/2$ cells form a *leading window*. Two statistics U and V are obtained from the sum of the contents of the leading and the lagging windows respectively. Then U and V are combined to obtain the estimate of the background noise power level Z as shown in Fig. 2-12. The statistic Z is then multiplied by a scaling factor T , called the threshold multiplier, to obtain the adaptive threshold for the design probability of false alarm. Normally, the threshold multipliers are computed tabulated in a look-up table for the desired probability of false alarm. Then the CUT is compared with the adaptive threshold to make the decision whether a target is present or not. The performance of the CA-CFAR detector is optimum in a homogeneous environment that is when the noise samples of the reference cells are independent and identically distributed. As the number of reference cells increases, the detection performance of the CA-CFAR approaches that of the classical Neyman-Pearson detector which is optimal when the noise power is known [8, 10].

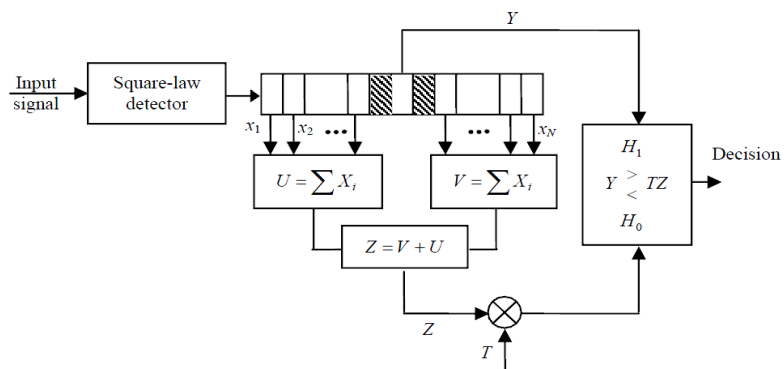


Fig. 2-12: Cell averaging CFAR [8].

In non-homogeneous environments, presence of clutter edge and/or presence of interfering targets, the performance of the CA-CFAR detector is seriously degraded. Clutter edge describes a situation where there is an abrupt transition in clutter power distribution within the reference window, while interfering targets describe a situation where there are interfering targets within the reference window. In this case, robust algorithms are needed to estimate the total noise power from the cells surrounding the CUT.

Clutter Edge model

It is assumed in this case that the total noise power as a function of range can be represented by step functions as shown in Fig. 2-13 and Fig. 2-14.

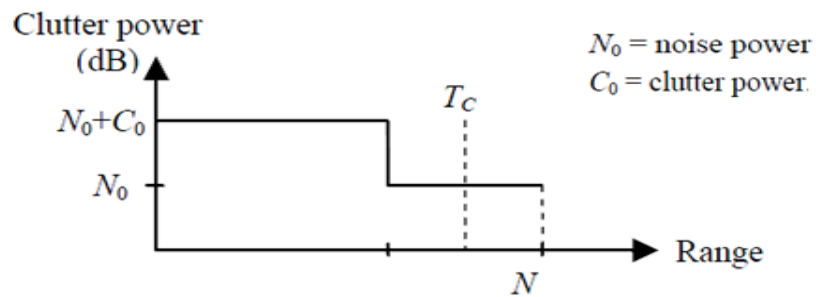


Fig. 2-13: Model of a clutter edge where test cell in clear [8].

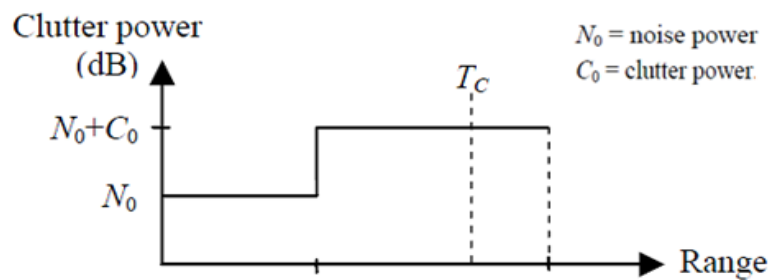


Fig. 2-14: Model of a clutter edge where test cell in clutter [8].

The presence of clutter edge may result in a severe degradation of the detector performance, which may cause excessive false alarms or a masking effect depending on whether the CUT is in the clear or clutter region. If the CUT is in the clear but a group of reference cells are immersed in the clutter as shown in Fig. 2-13. A masking effect for the target in the CUT will result due to the raising of the adaptive threshold value. Thus, the probability of detection is reduced as well as the probability of false alarm. Trunk [46] proposed the smallest-of-selection logic in cell averaging constant false-alarm rate detector (SO-CFAR) where the minimum of U and V is selected to represent the noise level estimate in the CUT, i.e. $Z = \min(U, V)$. If the CUT is immersed in the clutter but some of the reference cells are in the clear region as shown in Fig. 2-14, the adaptive threshold value is relatively low and the probability of false alarm increases. Hansen and Sawyers [47] proposed the greatest-of-selection logic in cell averaging constant false-alarm rate detector (GO-CFAR) to control this increase in the probability of false alarm. In the GO-CFAR detector, the estimate of the noise level in the CUT is selected to be the maximum of U and V , that is $Z = \max(U, V)$.

Homogeneous Background plus Interfering Targets

This model describes the situation where the background is composed of homogeneous white Gaussian noise plus interfering targets. The targets appear as spikes in individual range cells and it may fall in either the leading or lagging windows, or in both windows at the same time. The presence of the interfering targets in the reference cells of the target under consideration, the primary target, will raise the adaptive threshold value and the detection of the primary target is seriously degraded. This is known as the capture effect. With the threshold too high, some targets may be undetected as illustrated in Fig. 2-15. On the other hand, if the threshold is not high enough as illustrated in Fig. 2-16, the number of false alarms due to noise spikes will increase.

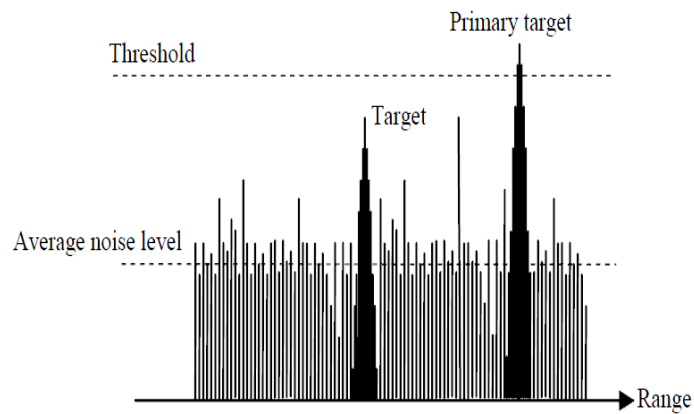


Fig. 2-15: Threshold too high [8].

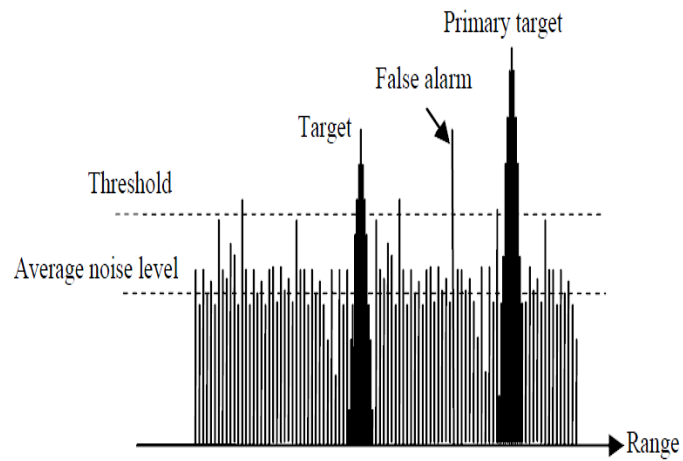


Fig. 2-16: Threshold not high enough [8].

To alleviate such problems, many CFAR detectors have been proposed in the literature [11-23]. The CMLD-CFAR, the TM-CFAR, and the OS-CFAR detectors have been stated in Chapter 1 are all examples of CFAR processing for this model.

Clutter Edge and Spikes

This model describes a situation where there is a transition in the clutter power distribution and interfering targets are present in the reference window as illustrated in Fig. 2-17.

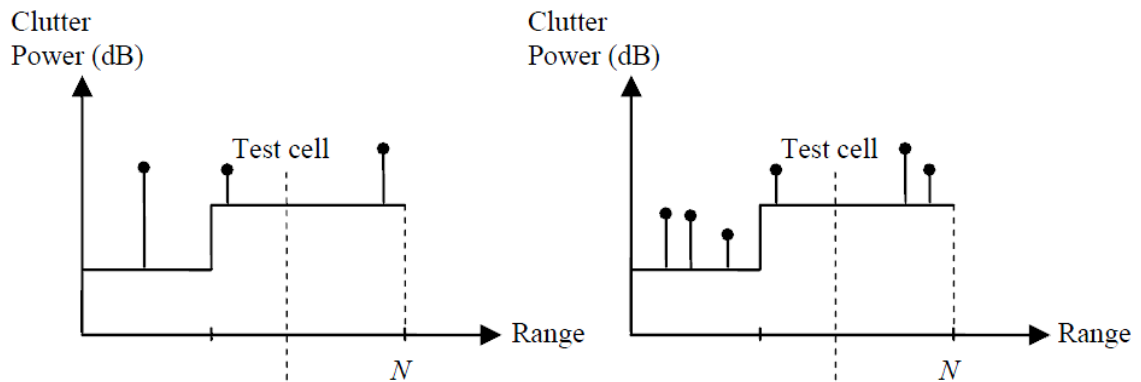


Fig. 2-17: The clutter edge and spikes model [8].

When both interfering targets and clutter edge are present in the reference window of the CUT, Himonas and Barkat [17] have proposed the generalized two-level censored mean level detector (GTL-CMLD) which uses an automatic censoring algorithm of the unwanted samples in order to compute the appropriate adaptive threshold level.

Non-Gaussian Noise

This model describes the situation that certain types of clutters are represented by non-Gaussian distributions, such as sea clutter, land clutter, and weather clutter. The log-normal, Weibull, and gamma distributions have been used to represent envelope-detected non-Gaussian clutter distributions.

2.5.2 Adaptive CFAR thresholding for the PN code acquisition

For adaptive PN acquisition in CDMA communication systems, the correlator outputs are sent serially into a shift register of length $N_c + 1$. The first register represents the CUT which contains the correlator output of the current examined phase while the N_c registers represent the cells of reference window containing the outputs of the previous N_c phases. The contents of the reference cells are used to get a statistic to represent the power-level estimate of the background noise, which is then multiplied by a constant scale factor to achieve the desired probability of false alarm as shown Fig. 2-18 [8].

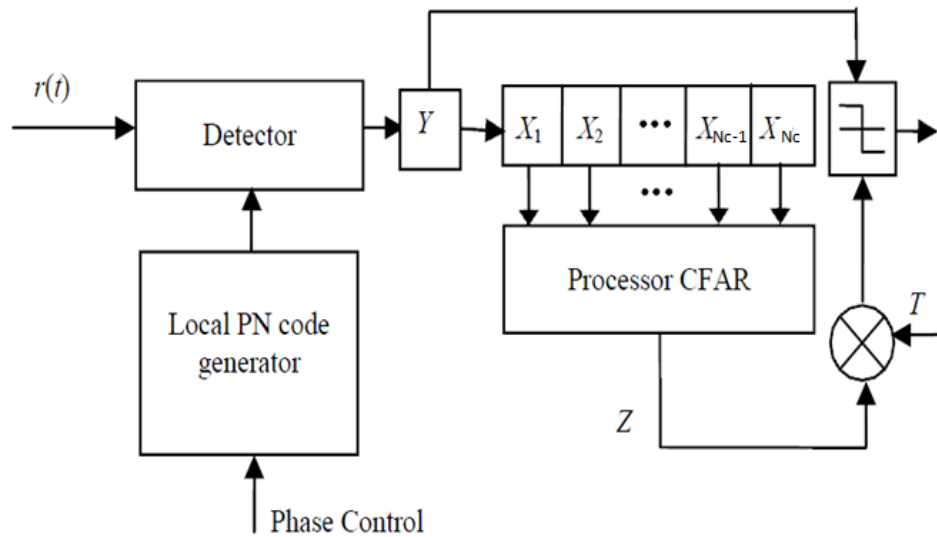


Fig. 2-18: Adaptive PN code acquisition detector

2.6 Smart Antenna Systems

The technology of smart antennas for mobile communications has received enormous interest worldwide during the last few years. It might seem that smart antenna is a new technology; but in fact, the fundamental principles upon which it is based have been applied in defense related systems since World War II. As a result of the emergence of powerful low cost digital signal processors, general purpose processors and application

specific integrated circuits (ASICs), as well as innovative software based signal processing algorithms; smart antennas have become practical for commercial use [48-49].

2.6.1 What is the Smart Antenna System?

A smart antenna system is an array of antenna elements with a digital signal processing (DSP) unit that automatically optimizes its radiation or/and reception pattern in response to its signal environment in order to emphasize signals of interest and to minimize interfering signals. Having an adaptive pattern is the property that distinguishes smart antennas from the fixed antennas which have a fixed pattern.

Using a fixed antenna in base stations has some disadvantages; most of the base station's power is wasted in radiation in other directions than toward the intended user. Also, this radiated power in the other directions will be considered as interference by other users. Smart antennas exploit the idea that interferers rarely have the same geographical location as the user. So, by maximizing the antenna gain in the desired direction and simultaneously placing minimal radiation pattern in the directions of the interferers, the quality of the communication link can be significantly improved. Using smart antennas will lead to a much more efficient use of the power and spectrum, increasing the useful received power as well as reducing interference [48, 50].

To easily understand the functionality of a smart antenna system, an example from the reality is given. There is a similarity between the idea of a smart antenna system and the human auditory system. Let us imagine some people carrying on a conversation and there is a blind person. We will find this person has the capability of determining the location of the speaker as he moves. This is because the voice of the speaker arrives at

each ear at a different time, so the brain can compute the direction of the speaker from the time differences or delays received by the two ears. Afterwards, the brain adds the strength of the voice signals from each ear, so as to focus on the sound of the computed direction. Moreover, if there are many people talking simultaneously, the brain has the ability to enhance the received signal from the speaker of interest and attenuate unwanted interferers so the person can concentrate on one conversation at a time as shown in Fig. 2-19. By using antennas instead of the ears and a digital signal processor instead of the brain, the smart antenna system works in the same way [51].

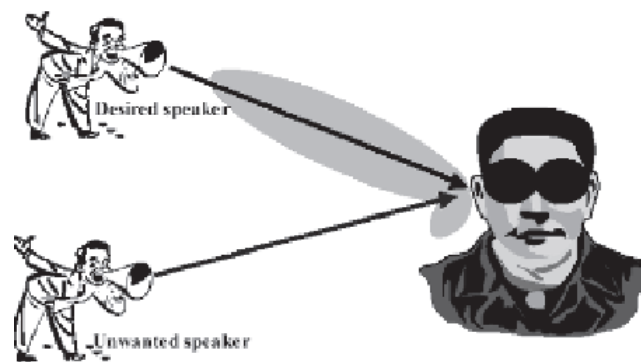


Fig. 2-19: Human auditory function [51].

2.6.2 Architecture of the Smart Antenna System

In this section, we give an overview of the architecture of a smart antenna system for reception and transmission of signals as shown in Fig. 2-20. It consists of multiple antenna elements, a DSP unit, which can be divided into a beamforming network and a signal processing unit, and a radio unit. The array of antennas consists of M antenna elements. The antenna in the telecommunication systems can be defined as the device through which, in the receiving mode, radio frequency (RF) energy is coupled from the outside world to the receiver and from transmitter to the outside world in the transmission mode. These antenna elements can be arranged in various physical

arrangements such as linear, circular, and rectangular. The radio unit consists of down-conversion chains and an analog-to-digital (A/D) conversion unit following each antenna element [51].

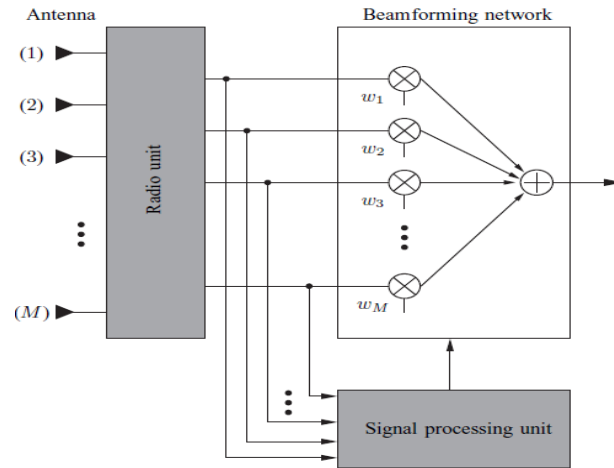


Fig. 2-20: Reception part of the smart antenna system [51].

The received signal at the different antenna elements is down-converted to baseband and digitized. It is multiplied with complex weights which adjust its phase or/and its amplitude and then all weighted signals are combined as a one input to the remaining part of the receiver. The optimum weights are computed by the signal processing unit which applies an adaptive beamforming algorithm, which will be explained in the next section. These optimum weights will determine the optimum antenna pattern in the uplink direction [51].

The transmission part of a smart antenna system is similar to the reception part as shown in the Fig. 2-21. The radio unit consists of a digital-to-analog (D/A) converter and the up-converter chains for each antenna elements. In the beamforming network, the signal is weighted by the complex weights after it has been split into N branches. These

weights are computed by the signal-processing unit to form the optimum radiation pattern in the downlink direction [51].

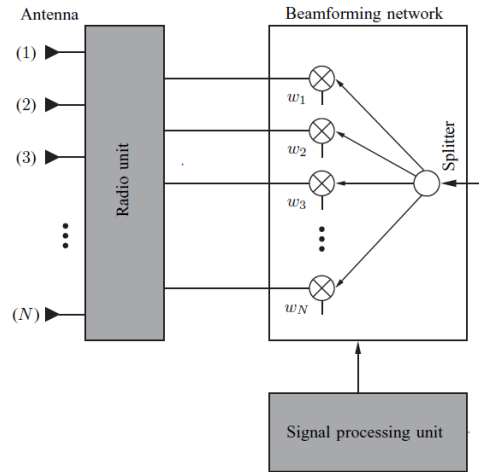


Fig. 2-21: Transmission part of a smart antenna.

2.6.3 Adaptive Beamforming Algorithms

Adaptive beamforming algorithms provide smart antenna systems with the unique ability to alter the radiation and reception pattern characteristics (main beam direction, nulls, sidelobe level, and beamwidth). They calculate the weights for each antenna element of the array in order to optimize some properties of the received signal. Many algorithms include optimization procedures based upon certain criteria. The most popular optimization criteria are: (1) maximum signal-to-interference plus- noise ratio (SINR) and (2) squared function based criteria such as mean square error (MSE), (3) minimum variance (MV), and (4) maximum likelihood (ML) [51-52].

There are two main strategies for the adaptive beamforming algorithms. The first strategy is based on the assumption that part of the desired signal is already known through the use of a training sequence. By comparing the known signal with the

received signal, the weights are adjusted to optimize the selected criteria such as minimization of the MSE between the known and the received signals. This way, the beam pattern can be adjusted to null the interferers. This approach optimizes the signal-to-interference ratio (SIR), and is applicable to non-line-of-sight (NLOS) environments. Since the weights are updated according to the incoming signals, not only the interference is reduced but the multipath fading is also mitigated. In the second strategy there is no need for the training sequence, it is based on identifying the direction of arrival (DOA) of the received signals firstly by using one of the DOA estimation methods such MUSIC (Multiple Signal Classification) and ESPRIT (Estimation of Signal Parameters via Rotational Invariant Techniques) among many others. The beamforming process is done by adjusting the weights to direct the main beam toward the desired user and nulls toward interfering signals. In practical scenarios such as NLOS environments, where there are many local scatterers close to the users and the base station, this strategy may turn out to be deficient because there are too many DOAs due to multipath, and the algorithms are more likely to fail in properly detecting them [51].

2.6.4 Types of the Smart Antenna Systems

Smart antenna systems can be classified into two main categories based on how they produce their beam pattern; switched beam as shown in Fig. 2-22 (a) or adaptive array as shown in Fig. 2-22 (b).

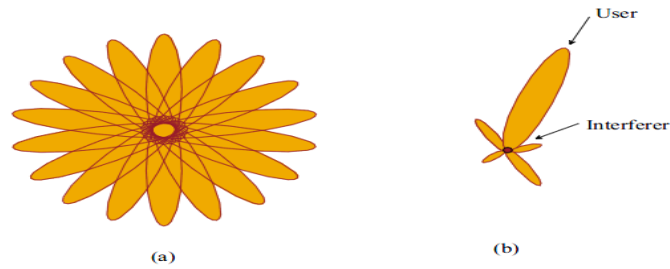


Fig. 2-22: Coverage pattern: (a) switched beam, (b) adaptive array [50].

Switched Beam System

The switched beam system is the simplest smart antenna system. Multiple fixed beams are formed by a beamforming network then the beam giving the strongest received signal is selected. Such type of smart antenna system detects the signal strength, chooses from one of the available beams, and as the user moves it switches from one beam to another as shown in Fig. 2-23. The overall goal of this system is to increase the gain according to the location of the user [49, 51].

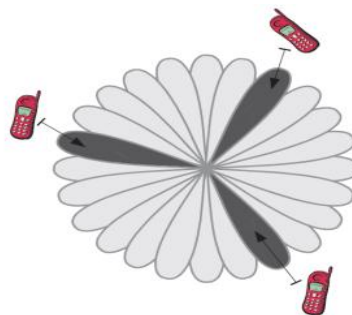


Fig. 2-23: Switched beam smart antenna system [51].

In terms of radiation patterns, the switched beam system is an extension of the current cellular sectorization method as each macro-sector is further subdivides into several micro-sectors. Each micro-sector contains a predetermined fixed beam pattern

with the greatest sensitivity located in the center of the beam and less sensitivity elsewhere [50].

Adaptive Array System

The adaptive array system is the most advanced smart antenna systems. This type of smart antenna systems continuously adjusts and changes its beam pattern to enhance the reception of the desired signal while minimizing interference through using signal processing algorithms. It directs the main beam toward the pilot signal and the signal of interest (SOI), while the side lobes and the nulls of the beam pattern are placed in the direction of the interferers or signals not of interest (SNOIs). The beam can be steered toward a desired direction by applying phase weighting on the outputs of the array elements and can be shaped by amplitude and phase weighting [49, 51].

In general both systems direct the beam (main lobe) toward the direction of the desired signal and attempt to minimize and reject the interference signals, but the adaptive array system does that in an efficient manner. Since the beams are fixed and predetermined in the switched beam system, the strength of the desired signal varies as the user moves through the active beam. The signal strength can degrade rapidly as the user moves towards the far azimuth edges of a beam. The switched beam system is not only unable to direct the maximum of the main lobe toward the desired signal, but it also shows inability to fully reject interference signals and distinguish between the desired signal and interfering ones as shown in see Fig. 2-24. It suppresses interference arriving from directions away from the active beam. But if the interfering signal is at approximately the center of the active beam and the user is away from the center of the beam, the interfering signal will be enhanced far more than the desired signal so the quality for the signal is degraded. On the other hand, the adaptive array system has the ability to control the overall beam pattern and for that it offers substantial performance

advantages over the passive switched beam system. As mentioned previously, this system has the ability to locate and track users and interferences signals and dynamically adjust the antenna beam pattern to enhance reception while minimizing interferences. As shown in Fig. 2-24, it chooses a more accurate placement, thus providing greater signal enhancement [49, 51].

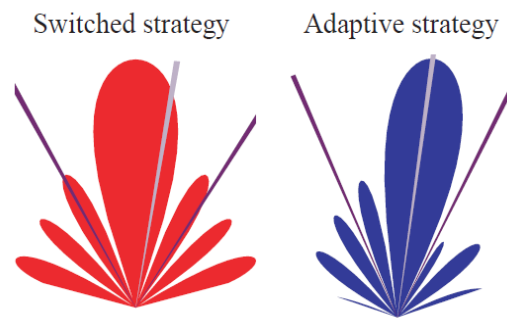


Fig. 2-24: Switched beam and adaptive array beams in the presence of interference signals [51].

Both types of smart antenna systems provide significant gains over conventional sectorized systems in the low interference environment. However in the environment with a significant level of interference, the interference rejection capability of the adaptive array system provides significantly more coverage than either the conventional or switched beam systems, see Fig. 2-25 [51].

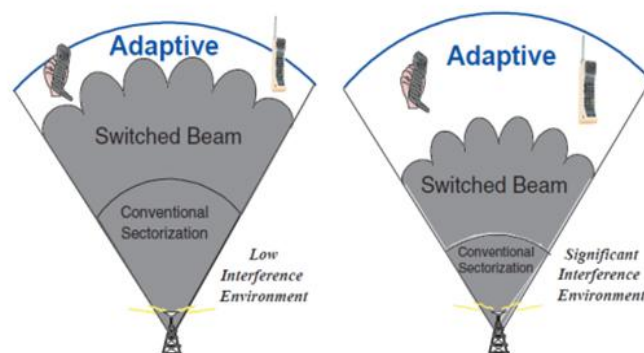


Fig. 2-25: Switched beam and adaptive array coverage in low/significant interference environment [51].

2.6.5 The Advantages of the Smart Antenna Systems

The main impediments to high performance wireless communications are the interference from other users (co-channel interference), and the multipath signals that cause the inter-symbol interference (ISI) and signal fading. As explained earlier, smart antenna exploits the idea that the desired signal and multipath and interference signals typically arrive at the receiver from different directions. So by directing the radiation pattern toward the desired users and trying to placing nulls in the directions of all unwanted interference, the useful received signal level will be increased and the interference level will be lowered which leads to increasing the SIR. Also by using multiple antennas, more signal energy will be captured which can be combined to improve the signal-to-noise ratio (SNR) [49, 53].

The introduction of smart antenna in wireless communication has a large impact on the performance of these communication systems. In the following some of the benefits that will be gained from employing smart antenna in wireless communication:

- *Reducing Multipath Effects:* by focusing the beam on the intended user, the ISI effect due to the multipath propagation is mitigated [51].
- *Capacity Increase:* In densely populated areas, the interference from other users is the main source of noise in the communication system. These co-channel interferences limit the wireless communication capacity, which is defined as the number of users which can be serviced by the system. Since smart antenna can reduce the co-channel interference, the system capacity will be increased [48, 53].
- *Range Increase:* In rural and sparsely populated areas, an increase of the range of coverage by a base station is an important issue. Since smart antenna is more

directive than traditional sector or omnidirectional antennas, increasing the range is possible [48].

- *Security:* another added benefit for the directivity feature of a smart antenna is the security. Using a smart antenna makes it more difficult to tap a connection. Because to successfully tap a connection the intruder must be positioned in the same direction as the user as seen from the base station [48].
- *Others Services:* also due to the spatial directivity feature of smart antennas, it becomes possible to have access to spatial information about the users. This information can be used to estimate the positions of the users which will help in services such as emergency calls and location specific billing [48].

Chapter 3

Communication System Model and Analysis

Summary

In this chapter, we describe the proposed wireless communication system which was first introduced by Sofwan and Barkat in [1], and which adopts smart antenna and adaptive thresholding CFAR detection. The CMLD-CFAR processor is considered for CDMA PN acquisition. We derive closed form mathematical expressions for the probability of false alarm, the probability of detection, and the mean acquisition time. The performance of the considered wideband communication system is investigated and analyzed. Simulation results show that the system under consideration is robust in a real multipath environment.

3.1 Introduction

3.2 Communication System Model

3.3 System Analysis

3.4 Results and Discussions

3.1 Introduction

In [1], Sofwan and Barkat proposed a novel idea of using smart antennas and adaptive thresholding CFAR detection for PN acquisition in wireless DS-CDMA communication systems in a slowly fading multipath and multiple access interference channel environment. They considered the trimmed mean constant false alarm rate (TM-CFAR) detector for PN acquisition. In [35] a system utilizing an LMS algorithm for adaptive beamforming and a fixed threshold with smart antenna was proposed for wireless communication. They showed that smart antenna shorten the acquisition time and improve the detection probability as compared to a single antenna element. In [37], Puska et *al.* considered an approach where the direction of arrival (DOA) estimation and beamforming of the incoming signal are combined with a fixed threshold detector for code acquisition in a spread spectrum communication system. They showed that the mean acquisition time achieved by DOA estimation is shorter than that achieved by fixed beamforming.

As mentioned earlier, in a real mobile communication environment with multipath and multiple access interference, and due to variations in the received power caused by the influence and mobility, adaptive CFAR thresholding techniques are preferred. [54] suggested the use of a of an adaptive acquisition processor (AAP) for a known number of interferers, which they called excision cells. The processor in [54] is actually the CMLD proposed in [13]. Mathematical expressions for the probabilities of detection and false alarm were given in [27].

In this thesis we consider the communication system with smart antennas proposed in [1], but using instead a CMLD-CFAR adaptive thresholding processor. The CMLD-CFAR detector proved to be robust in an environment with multiple interfering

signals [13-14]. In addition, it was shown in [1] that the performance of the proposed communication system using the classical cell-averaging CFAR detection is equivalent to the system proposed in [35] in the presence of multipath and multiple access interference without resorting to robust order statistic CFAR detectors. In addition, [35] did not consider multiple access interference. The channel model assumed is a Rayleigh slowly fading multipath and multiple access interference communication channels. Closed form expressions for the probability of false alarm, the probability of detection, and the mean acquisition time are derived. Then the performance of the PN acquisition is investigated and analyzed for different design parameters of the communication system under consideration.

3.2 Communication System Model

The block diagram of the proposed PN acquisition system for wideband communication is shown in Fig. 3-1. The system consists of a smart antenna with M antenna elements; each antenna element followed by a correlator that correlates the received PN code sequence with the locally generated PN code sequence. The outputs of the M correlators serve as inputs to the LMS processor to update the smart antenna's weight vector. After getting the optimum weight vector, the spatial correlation outputs from the LMS are fed into the CMLD-CFAR processor, which is a tapped delay line, to set the threshold adaptively in order to make a final decision about whether there is acquisition or not.

D users

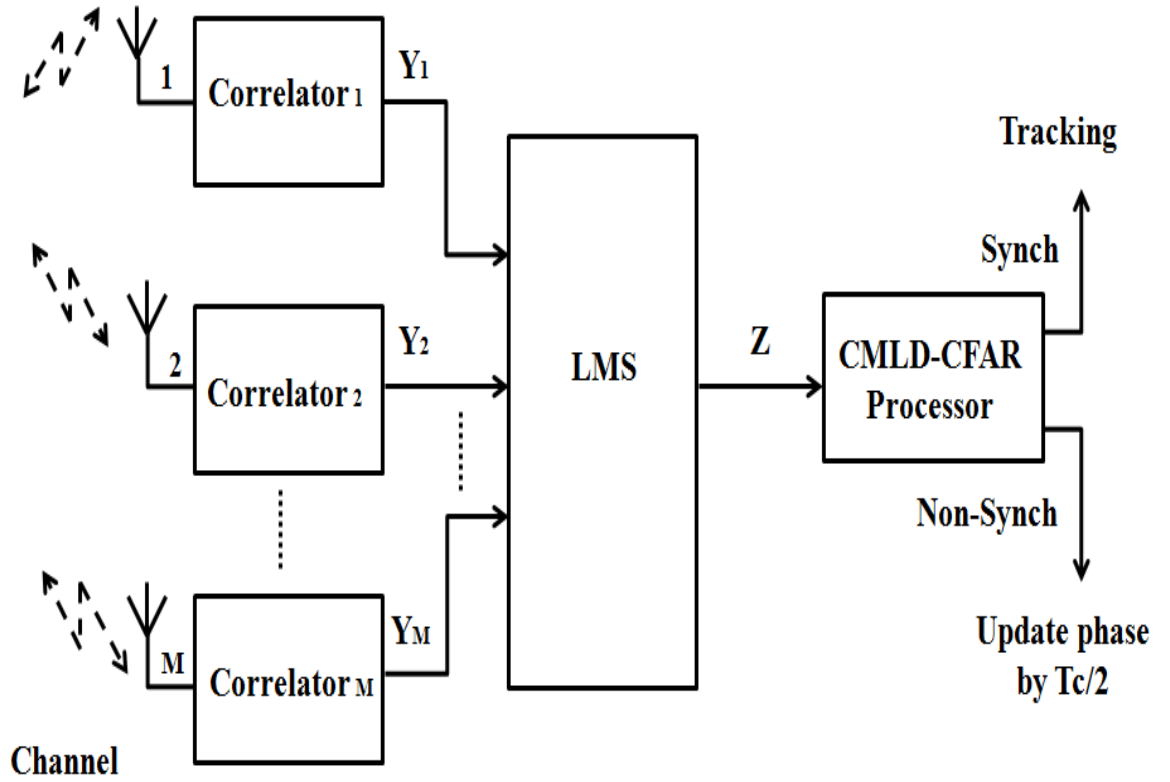


Fig. 3-1: Block diagram of the proposed communication system.

In this communication system we assume that there are D users from simultaneous transmitters. The first user is an initial synchronization user whose performance is to be evaluated, while the other $D - 1$ users are data transmission users who have finished acquisition and considered as interferers to the first user.

3.2.1 The Transmitted Signal

The transmitted signal of the i^{th} user, where $i = 1, \dots, D$, is given by [4]:

$$s_i(t) = \sqrt{2P_{T_i}} d_i(t) c_i(t) e^{j(\omega_c t + \xi_i)} \quad (3.1)$$

where P_{T_i} is the transmitted power of the i^{th} signal, d_i is the data signal, c_i is the PN code spreading sequence, ω_c is the angular carrier frequency, and ξ_i is the phase of the i^{th} modulator from the transmitter. It is assumed that no data signal is sent during the acquisition process (i.e. $d_1(t) = 1$).

3.2.2 The Communication Channel Model

The user signals are sent through a communication channel assumed to be a Rayleigh slowly fading multipath channel. The communication channel model considered consists of L tapped delay lines that correspond to the number of resolvable multipath with amplitude α_{il} and phase ζ_{il} , $l=0, \dots, L-1$, as shown in Fig. 3-2. α_{il} are independent and identically distributed (i. i. d.) Rayleigh random variables with a probability density function (pdf) [1]:

$$f_{\alpha_{il}}(x) = \frac{2x}{\Psi} e^{-\frac{x^2}{\Psi}}, \quad x \geq 0 \quad (3.2)$$

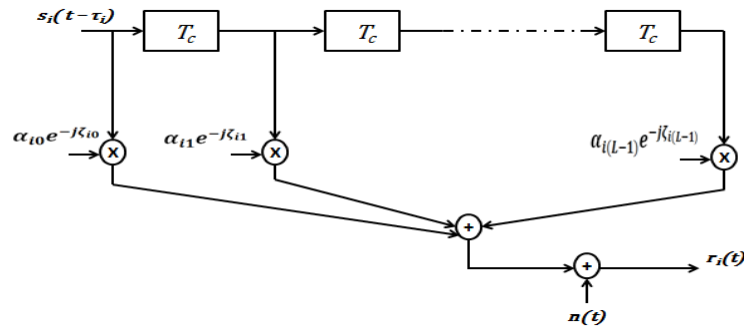


Fig. 3-2: Tapped delay line model of the frequency-selective channel.

where $\Psi = E[\alpha_{il}^2] = 2\sigma_f^2$, and σ_f^2 is the Rayleigh fading channel power. The phases ζ_{il} are independent and identically distributed random variables uniformly distributed in $[0, 2\pi]$. The fading amplitude is assumed to be constant during an observation interval but changes from one interval to another independently.

3.2.3 The Antenna Array Elements

The receiving antenna array is a uniform linear array (ULA) antenna consists of M identical elements spaced d apart, where $d = \lambda_c/2$ and λ_c is the wavelength of the carrier transmitted signal. Hence, the response vector of the antenna array to the first user signal can be expressed as [51]:

$$\mathbf{a}(\theta) = [1 \quad e^{-j\pi \sin \theta} \quad \dots \quad e^{-j\pi(M-1)\sin \theta}]^T \quad (3.3)$$

where $\mathbf{a}(\cdot)$ is the array vector of antenna, θ is the DOA angle of the desired signal, and T denotes transpose. The antenna considers a zero-beam spread angle model. LMS is the adaptive array antenna algorithm which will be used to adapt iteratively its weight vector to the array response vector. The vector array response is not a main concern in this thesis.

3.2.4 The Received Signal

Taking into account the effect of multipath, the received signal $r_m(t)$ for the m^{th} antenna element of the array is given in (3.4) [55], where $m = 1, \dots, M$. It consists of the signal from the first user, multiple access interferences from the others, and an AWGN $n(t)$.

$$\begin{aligned} r_m(t) = & \sqrt{2P_s} \left\{ \sum_{l=0}^{L-1} \alpha_{1l} c_1(t - \tau_1 - lT_c) e^{j(\omega_c t + \phi_{1l} - \pi(m-1)\sin \theta)} \right\} \\ & + \sqrt{2P_I} \left\{ \sum_{i=2}^D \sum_{l=0}^{L-1} \alpha_{il} d_i(t - \tau_i - lT_c) c_i(t - \tau_i - lT_c) e^{j(\omega_c t + \phi_{il} - \pi(m-1)\sin \theta)} \right\} \\ & + n(t) \quad (3.4) \end{aligned}$$

P_s is the received signal power of the first user during initial synchronization, P_I is the average received power of the interfering signal, τ_i is the relative time delay associated with the asynchronous communication channel model, $\phi_{il} = \xi_i - \zeta_{il} - \omega_c(\tau_i + lT_c)$ is

phase in the demodulator of the receiver which are independent and identically distributed random variables uniformly distributed on the interval $[0, 2\pi]$, and T_c is the chip duration.

3.2.5 The Correlator

The correlator for the PN code acquisition that follows the m^{th} antenna element in the system is shown in Fig. 3-3. The received signal is first down-converted into in-phase (I) and quadrature phase (Q) components. These components are then multiplied by the locally generated PN code $c(t - jT_c/2)$, $j = 0, 1, \dots, N_c$ (N_c represent the reference window size), and integrated over dwell time interval $\tau_D = RT_c$ seconds, where R is the correlation length integer, to yield respectively the I and Q branch components Y_{cjm} and Y_{sjm} , which are squared and summed to give the correlator output Y_{jm} , $Y_{jm} = |Y_{cjm}|^2 + |Y_{sjm}|^2$. The output Y_{jm} will be a high correlation value when the current delay of the local PN code (i.e. tested code phase) is a synchronized code phase cell with which the local PN code sequence is aligned with any of the multipath signals of the first user (H_1 hypothesis). Otherwise, it will be a negligible value due to the non-alignment case (H_0 hypothesis).

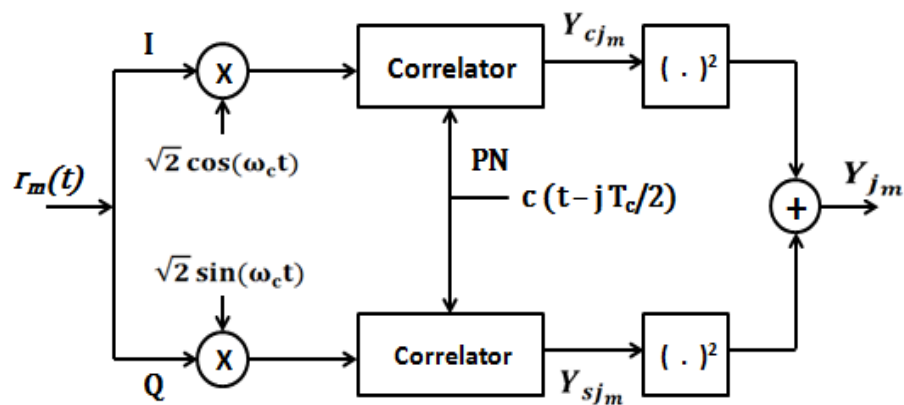


Fig. 3-3: Correlator consists of in-phase (I) and quadrature-phase (Q) components.

Due the Gaussian nature of Y_{cjm} and Y_{sjm} , and under the H_1 hypothesis for a given α_{1l} , the Y_{jm} will has a non-central Chi-square distribution with two degrees of freedom. The pdf of Y_{jm} can be written as [4, 8]:

$$f_{Y_{jm}|\alpha_{1l}}(y|\alpha_{1l}, H_1) = \frac{1}{2\sigma_0^2} e^{-\left(\frac{\lambda^2+y}{2\sigma_0^2}\right)} I_0\left(\frac{\lambda^2\sqrt{y}}{\sigma_0^2}\right), \quad y \geq 0 \quad (3.5)$$

where λ^2 is the normalized non-central metric given by $\lambda^2 = \frac{9}{16}\alpha_{1l}^2$, $I_0(.)$ is the zeroth-order modified Bessel function of the first kind, and σ_0^2 is the variance which is given by [4]:

$$\sigma_0^2 = \frac{(L-1)\Psi}{3R} + \frac{L(D-1)\beta\Psi}{3R} + \frac{1}{2RS_c} \quad (3.6)$$

β represents the average received power of the interfering signal to the signal power of the first user ratio and is defined as $\beta = P_I / P_s$, while S_c represents the $SNR/chip$ and is given by $S_c = T_c P_s / N_0$.

Under the H_0 hypothesis, the Y_{jm} will has a non-central Chi-square distribution with two degrees of freedom and its pdf is given as [4, 8]:

$$f_{Y_{jm}}(y|H_0) = \frac{1}{2\sigma_0^2} e^{-\left(\frac{y}{2\sigma_0^2}\right)}, \quad y \geq 0 \quad (3.7)$$

Since $f_{Y_{jm}}(y|H_1) = \int_0^\infty f_{Y_{jm}}(y|\alpha_{1l}, H_1) f_{\alpha_{1l}}(\alpha_{1l}) d\alpha$, then after some mathematical manipulations the pdf of the output Y_{jm} under the aligned hypothesis is given by [34]:

$$f_{Y_{jm}}(y|H_1) = \frac{1}{2\sigma_0^2(1+\nu)} e^{-\left(\frac{y}{2\sigma_0^2(1+\nu)}\right)}, \quad y \geq 0 \quad (3.8)$$

where $v = 9\sigma_f^2 / 32\sigma_0^2$.

3.2.6 The Least Mean Square Processor

The outputs $Y_{j_m}, m = 1, 2, \dots, M$, from the M correlators are inputs to the LMS processor as shown in the following figure.

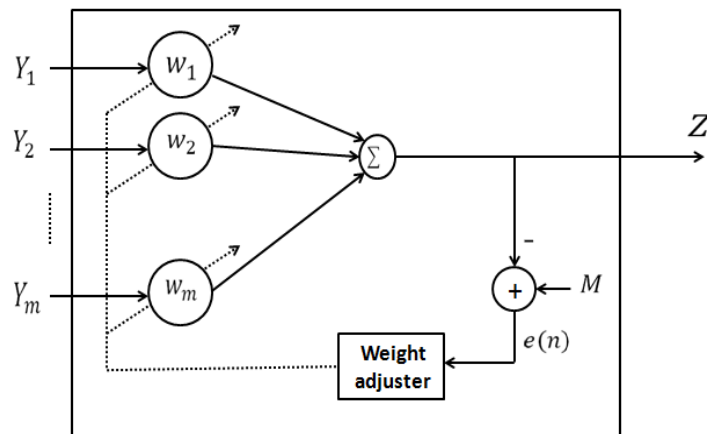


Fig. 3-4: The LMS processor.

The LMS algorithm computes iteratively the optimum weight vector in order to obtain a spatial correlation output that achieve the minimum MSE between the desired value and the LMS processor output. The weighting of the LMS processor maximizes the output by adapting the weights $w_m, m = 1, 2, \dots, M$ directly proportional to the step size parameter. The step size is assumed to be $\mu = 1/M$ for achieving convergence. Moreover, the optimum weight is assumed to be achieved when the power of the desired signal equals to M . Thus, the value of the error signal that is used by the LMS processor to adjust the weights adaptively in the n^{th} iteration is $e(n) = M - w_v^H(n)Y_v(n)$, where Y_v and w_v are vectors of the correlator outputs and weights respectively. The iterative procedure of LMS processor is given by [1]:

$$w_v(n+1) = w_v(n) + \mu e^*(n)Y_v(n) \quad (3.9)$$

Once the minimum MSE is attained, then this weight vector is used to generate the spatial correlation output Z . In the aligned hypothesis, it is assumed that the DOA of the desired signal can be located optimally by the smart antenna and the pdf of the Z under the aligned hypothesis is given as [1]:

$$f_Z(z|H_1) = \frac{1}{2\sigma_0^2(M + M^2\nu)} e^{-\left(\frac{z}{2\sigma_0^2(M + M^2\nu)}\right)} \quad , \quad z \geq 0 \quad (3.10)$$

While under the non-aligned hypothesis, it is assumed that the smart antenna tracks in a different angle than the desired signal and the pdf of Z is given as [1]:

$$f_Z(z|H_0) = \frac{1}{2\sigma_0^2 M} e^{-\left(\frac{z}{2\sigma_0^2 M}\right)} \quad , \quad z \geq 0 \quad (3.11)$$

3.2.7 The CMLD-CFAR Processor

The outputs of the LMS processor are serially fed into a shift register of length $N_c + 1$ as shown in Fig. 3-5. The first register, denoted as Z_0 , stores the current output of the LMS processor. The following N_c registers, denoted by $Z_c, c = 1, 2, \dots, N_c$ are the reference cells. First, Z_c 's are ranked in ascending order according to their magnitude to form the ordered samples $Z_{(1)} \leq Z_{(2)} \leq \dots \leq Z_{(N_c)}$, where $Z_{(j)}, j = 1, 2, \dots, N_c$ represent the order statistics of the Z_c samples. Then the k largest ranked cells are censored, where k is number of H_1 cells that result from the alignment of the first user multipath signals, and the remaining ones are combined to yield an estimate of the background noise level U .

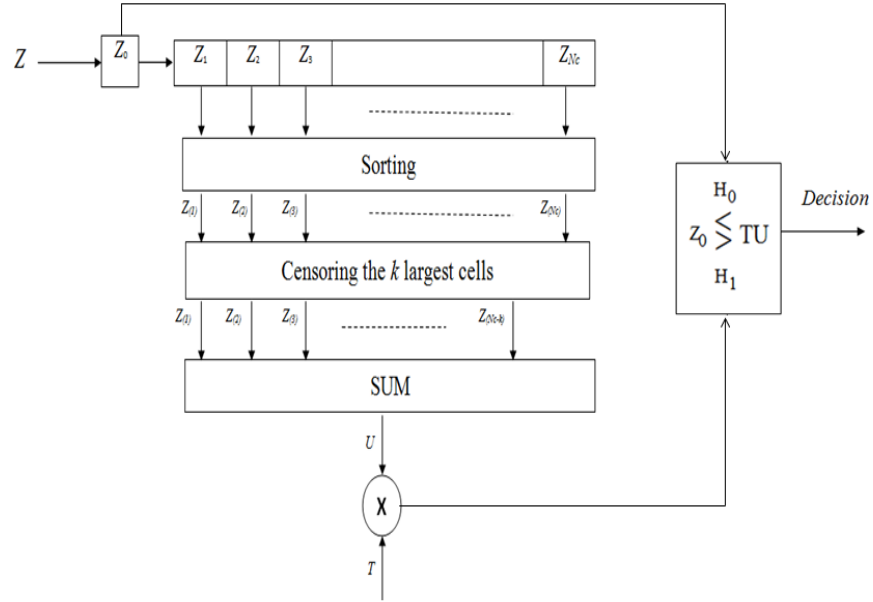


Fig. 3-5: CMLD-CFAR processor.

$$U = \sum_{j=1}^{N_c-k} Z_{(j)} \quad (3.12)$$

After that the U value is scaled by the threshold multiplier T to achieve the design false alarm probability. If Z_0 is larger than the threshold TU , a PN code acquisition is declared, and the tracking loop is triggered. Otherwise, the acquisition scheme shifts the locally generated PN code phase and the search continue until a correct PN code phase is found.

3.3 System Analysis

In this section, we derive closed form expressions for the probability of false alarm, the probability of detection, and the mean acquisition time in order to study and analyze the PN acquisition performance of the proposed system.

3.3.1 The Probability of False Alarm

As shown in Chapter 2, the probability of false alarm is the probability that a correlation of a non-synchronized tested code phase pass the threshold value. It is given as:

$$P_{fa} = E_U[P(Z_0 > TU | H_0)] = M_U \left[\frac{T}{2\sigma_0^2 M} \right] = M_U \left[\frac{T}{a} \right] \quad (3.13)$$

where M_U is the moment generation function (MGF) of the estimate U and $a = 2\sigma_0^2 M$.

The ordered samples $Z_{(1)}, Z_{(2)}, \dots, Z_{(N_c-k)}$, are not i.i.d. random variables even when the original samples $Z_c, c = 1, 2, \dots, N_c$, are i.i.d. random variables. However, since that the i.i.d. Z_c samples are exponentially distributed, the following transformation to random variables $W_1, W_2, \dots, W_{N_c-k}$ results in independent quantities [15]:

$$\begin{aligned} W_1 &= Z_{(1)} \\ W_2 &= Z_{(2)} - Z_{(1)} \\ &\dots \\ &\dots \\ W_{N_c-k} &= Z_{(N_c-k)} - Z_{(N_c-k-1)} \end{aligned} \quad (3.14)$$

It is known that the pdf of order statistics $X_{(j)}$ of random variables X_1, \dots, X_N is given as [56]:

$$f_{X_{(j)}}(x) = \frac{N!}{(j-1)!(N-j)!} f_X(x) [F_X(x)]^{j-1} [1 - F_X(x)]^{N-j}, \quad j = 1, \dots, N \quad (3.15)$$

where $F_X(x)$ is the cumulative distribution function. So the pdf of W_1 is:

$$f_{W_1}(z) = \frac{N_c}{a} e^{-\frac{z N_c}{a}} \quad (3.16)$$

In the case of an exponential distribution the distributions of $X_{(j)} - X_{(j-1)}, j = 2, \dots, N$, are identical to the first order statistic $X_{(1)}$ of random variables $X_i, i = 1, \dots, N - j + 1$

[57]. By using this relation and (3.15), the pdf of the i.i.d. random variables W_2, \dots, W_{N_c-k} is as following:

$$f_{W_i}(z) = \frac{N_c - i + 1}{a} e^{\frac{-z(N_c-i+1)}{a}}, \quad i = 2, \dots, N_c - k \quad (3.17)$$

Let us define another transformation:

$$V_i = (N_c - k - i + 1) W_i, \quad i = 1, \dots, N_c - k \quad (3.18)$$

The random variables V_i 's are independent since W_i 's are independent. Thus the estimate U is given by:

$$U = \sum_{j=1}^{N_c-k} V_j \quad (3.19)$$

The V_i 's are functions of random variables W_i 's in the form $V_i = c_i W_i$, where $c_i = N_c - k - i + 1$, therefore, the pdf of the V_i is given as [8] :

$$f_{V_i}(z) = \frac{1}{c_i} f_{W_i}\left(\frac{z}{c_i}\right) \quad (3.20)$$

From (3.16), (3.17), and (3.20), the pdf of the V_i 's random variables is as following:

$$f_{V_1}(z) = \frac{N_c}{a(N_c - k)} e^{\frac{-z N_c}{a(N_c - k)}} \quad (3.21)$$

and

$$f_{V_i}(z) = \frac{N_c - i + 1}{a(N_c - k - i + 1)} e^{\frac{-z(N_c-i+1)}{a(N_c-k-i+1)}}, \quad i = 2, \dots, N_c - k \quad (3.22)$$

The MGF of U is simply the product of the individual MGF of V_i 's. Therefore the probability of false alarm is:

$$P_{fa} = \prod_{i=1}^{N_c-k} M_{V_i}\left(\frac{T}{a}\right) \quad (3.23)$$

where

$$M_{V_1}\left(\frac{T}{a}\right) = \frac{N_c}{(N_c - k) \left(T + \frac{N_c}{N_c - k}\right)} \quad (3.24)$$

and

$$M_{V_i}\left(\frac{T}{a}\right) = \frac{g_i}{T + g_i} \quad , i = 2, \dots, N_c - k \quad (3.25)$$

and

$$g_i = \frac{N_c - i + 1}{N_c - k - i + 1} \quad (3.26)$$

3.3.2 The Probability of Detection

The presence of the multipath signals with the synchronization signal of the first user implies that there exist more than one possible synchronized code phase cells (offsets) in the uncertainty region. The probability of detection of the high correlation value that results of an alignment of the local PN code with any of the multipath signal under the current tested code phase is given by:

$$P_{d_l} = E_U[P(Z_0 > TU \mid H_1)] = M_U\left[\frac{T}{2\sigma_0^2(M + M^2v)}\right] = M_U\left[\frac{T}{b}\right], l = 0, \dots, L \quad (3.27)$$

where M_U is the MGF of the estimate U and $b = 2\sigma_0^2(M + M^2v)$. P_{d_l} is deduced in the same manner as P_{fa} and thus P_{d_l} is given by:

$$P_{d_l} = \prod_{i=1}^{N_c-k} M_{V_i}\left(\frac{T}{b}\right) \quad (3.28)$$

where

$$M_{V_1}\left(\frac{T}{b}\right) = \frac{bN_c}{aT(N_c - k) + bN_c} \quad (3.29)$$

and

$$M_{V_i}\left(\frac{T}{b}\right) = \frac{b(N_c - i + 1)}{aT(N_c - k - i + 1) + b(N_c - i + 1)} \quad , i = 2, \dots, N_c - k \quad (3.30)$$

3.3.3 The Mean Acquisition Time

The mean acquisition time is an important measure of the PN acquisition system performance. The acquisition time is the amount of time that elapses prior to acquisition i.e. locating the synchronization cell [3]. To derive the mean acquisition time (T_{acq}), the signal flow graph technique or sometimes called the state transition diagram is commonly used. In the following we will briefly introduce the state transition diagram for modeling the serial search acquisition process, and then the mean acquisition time of the proposed system is derived.

The serial search acquisition process can be modeled using the state transition diagram which is composed of a number of states or nodes connected by branches as shown in Fig. 3-6. The number of states used to model the process is a $v + 2$ states, where $v - 1$ of these states represent the non-synchronization cells (H_0 code phase offsets) while one state (the v th) is the collective state H_1 , thus any synchronization cells (H_1 code phase offsets) are included in this state. In addition to these v states of phase offsets, the remaining two states are: the False Alarm (FA) state which can be reached from any of the H_0 states and the correct Acquisition (ACQ) state which just can be directly reached from the v^{th} H_1 state. The v states are sorted in a circular arrangement with indices ($i = 1, 2, \dots, v - 1$) corresponding to the i^{th} offset code position to the right of the correct synchronization position H_1 . [3]

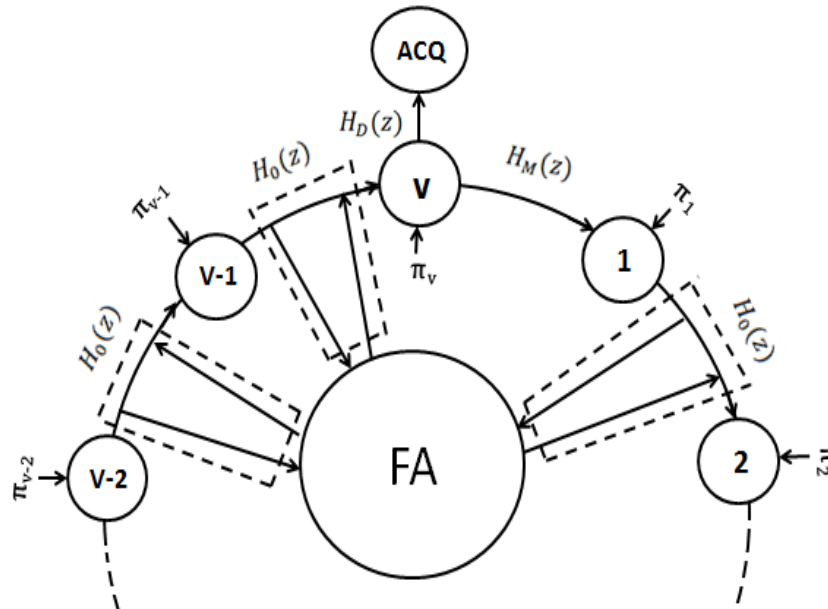


Fig. 3-6: The circular state transition diagram.

The searching process can start at any one of the v states, according to some a priori distribution $(\pi_j, j = 1, 2, \dots, v)$ which reflects the designer's confidence about the initial relative position of the codes. The branches are assigned gains or sometimes called transfer functions which contain information about the delays that may occur during the transition between two states as follows: $H_D(z)$ is the gain of the branch leading from the state H_1 to the ACQ state; $H_M(z)$ is the gain of the branch connecting H_1 with state or node 1 while $H_0(z)$ is the gain of the branch connecting any other two successive nodes $(i, i + 1)$; $i = 1, \dots, v - 1$. The transition from state i to state $i + 1$ can be performed without reaching the FA state when the examined i state showed it is a non-synchronization cell or the transition happened after first reaching the FA state when the examined i state (H_0 cell) give a false high correlation value, then the process passes from FA state to node $i + 1$ to complete the searching process [3, 45].

After the serial search acquisition process has been modeled by the state transition diagram, T_{acq} is derived from an expression of a generation or transfer function

$H(z)$ that is obtained from the state transition diagram. For our system, we used the following assumptions to derive T_{acq} :

- A uniform prior distribution which means that each node has the same probability for starting the search, $\pi_j = \frac{1}{v}$, $j = 1, 2, \dots, v$.
- The processing time of the LMS and the CMLD-CFAR does not affect the derivation of the mean acquisition time.
- We have used $1/2$ as a value of advancing the step size. So, the number of positions (cells of code phase offsets) to be tested is $q = 2\Theta$, where the Θ represent the total number of chips in the uncertainty region of T_u seconds. Therefore, v will be equal to $1 + (q - N)$, where $N = 2L$ is the number of synchronization cells (each resolvable path will contribute two synchronization cells).

The transfer functions $H_0(z)$, $H_D(z)$ and $H_M(z)$ of the state transition diagram are derived as follow:

- The transition from state i to state $i + 1$ can happen directly without reaching the FA state, this event will take a time equal to the dwell time interval τ_D with probability $(1 - P_{fa})$, or the transition after accessing the FA state occurs with probability P_{fa} . After the dwell time interval taken for a wrong decision, there is a penalty time for accessing the FA state and returning back to the search mode. We assume it is a constant time and equal to $p\tau_D$. Let z denote a unit-delay variable and let the power of z denote the time delay, then the function $H_0(z)$ can be expressed as [3]:

$$H_0(z) = (1 - P_{fa}) z^{\tau_D} + P_{fa} z^{(1+p)\tau_D} \quad (3.31)$$

- The collective H_1 state will have N synchronization cells, see Fig. 3-7. If $P_{d_j}, j = 1, \dots, N$ is the probability of detection of cell j within the collective H_1 state, the function $H_D(z)$ is given by [45]:

$$H_D(z) = P_{d_1} z^{\tau_D} + \sum_{j=2}^N P_{d_j} \left[\prod_{i=1}^{j-1} (1 - P_{d_i}) \right] z^{j\tau_D} \quad (3.32)$$

or can be written as :

$$H_D(z) = \sum_{j=1}^N P_{d_j} \left[\prod_{i=1}^{j-1} (1 - P_{d_i}) \right] z^{j\tau_D} \quad (3.33)$$

where $\prod_{i=1}^0 (1 - P_{d_i}) = 1$.

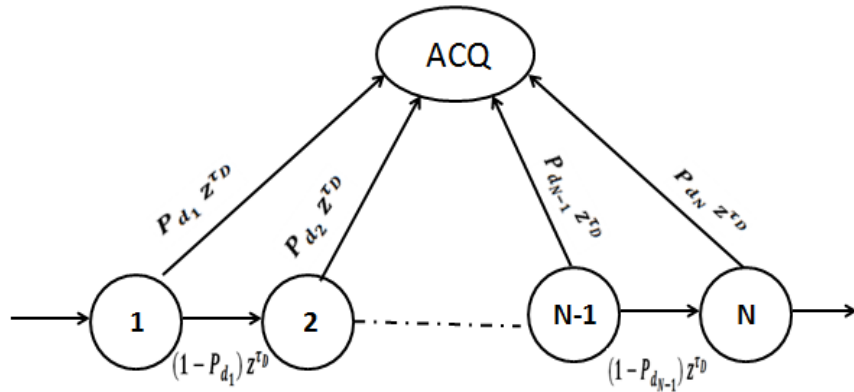


Fig. 3-7: The H_1 state.

- The function $H_M(z)$, which represents failure to recognize one of the N H_1 cells as a synchronization cell is given by [45]:

$$H_M(z) = \left[\prod_{j=1}^N (1 - P_{d_j}) \right] z^{N\tau_D} \quad (3.34)$$

For the single dwell serial search acquisition process with a uniform prior distribution, $H(z)$ is given by [3]:

$$H(z) = \frac{1}{v} \frac{H_D(z) (1 - H_0^v(z))}{(1 - H_M(z) H_0^{v-1}(z))(1 - H_0(z))} \quad (3.35)$$

The mean acquisition time is computed to be [3]:

$$T_{acq} = \left. \frac{dH(z)}{dz} \right|_{z=1} \quad (3.36)$$

When there is only one absorbing state which is the ACQ state. T_{acq} will then be [3]:

$$T_{acq} = \frac{1}{H_D(1)} \left[H'_D(1) + H'_M(1) + (v-1)H'_0(1) \cdot \left(1 - \frac{H_D(1)}{2} \right) \right] \quad (3.37)$$

Substituting Equations (3.31), (3.33) and (3.34) into (3.37), T_{acq} can be written as:

$$T_{acq} = \left[\frac{2 \sum_{j=1}^N j P_{d_j} [\prod_{i=1}^{j-1} (1 - P_{d_i})] + 2N [\prod_{j=1}^N (1 - P_{d_j})]}{2 \sum_{j=1}^N P_{d_j} [\prod_{i=1}^{j-1} (1 - P_{d_i})]} + \frac{(v-1)(1 + pP_{fa})(2 - \sum_{j=1}^N P_{d_j} [\prod_{i=1}^{j-1} (1 - P_{d_i})])}{2 \sum_{j=1}^N P_{d_j} [\prod_{i=1}^{j-1} (1 - P_{d_i})]} \right] \tau_D \quad (3.38)$$

3.4 Results and Discussions

In this section we present the MATLAB simulation results obtained of the wireless communication system considered in a Rayleigh slowly fading multipath channel.

3.4.1 Probability of Detection

For the simulation, the design probability of false alarm $P_{fa} = 10^{-3}$, the correlation length integer of the dwell time interval is set at value $R = 128$ and the number of reference cells is $N_c = 24$, unless otherwise stated. The values of these simulation parameters are same to what have been used in [1] and also they are used in many papers for simulation purpose. The threshold multiplier value T is readily obtained from the expression of the probability of false alarm given in (3.23). The interfering signals in the reference window are a result of multipath signals, MAI signals or a combination of them and for simulation the power of these simulated interfering signals is selected relative to the main signal power which is expressed by β (the average received power of the interfering signal to the signal power of the first user ratio).

It has been shown in [1] that the system proposed in [35] has the same performance as the system under consideration employing a smart antenna and an adaptive thresholding CA-CFAR processing with $N_c = 24$ reference cells. Fig. 3-8 shows that the detection performance of the system under consideration using CA-CFAR processing is seriously degraded in the presence of interfering signals. We observe that excision of interfering signals from the reference cells before estimating the noise power level improves the probability of detection. This is the essence the CMLD-CFAR detector.

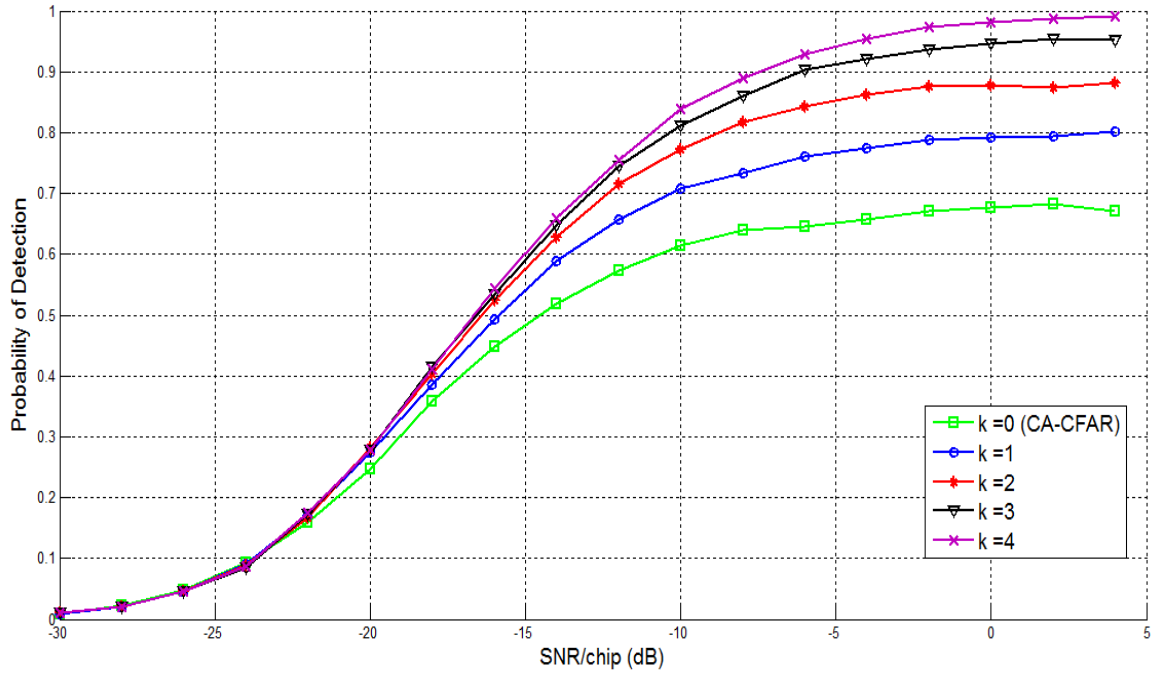


Fig. 3-8: Comparison of P_d using CA-CFAR processing with CMLD-CFAR system with interfering signals.

Fig. 3-8 shows the simulated detection probability P_d of the system against $SNR/chip$ under different numbers of censored cells k . The number of antenna elements used is $M = 3$ and the number of interfering signals is four, while the average received power of the interfering signal to the signal power of the first user ratio is $\beta = 0.3$. We observe that as the number of interfering signals censored increases, the detection performance improves as expected. This is due to the fact that the adaptive threshold computed after censoring becomes lower which yields a better detection probability. As we see, that all CMLDs ($k = 1, 2, 3$ and 4) have much better performance than the CA-CFAR ($k = 0$).

In Fig. 3-9 we plot the probability of detection P_d against the $SNR/chip$ of the proposed wideband communication system with smart antennas and the AAP system proposed in [27] without smart antenna. Both systems consider the CMLD-CFAR to compute the adaptive threshold. The number of antennas is $M = 1$ and 2 and three

interfering signals are assumed present and censored before computation of the adaptive threshold.

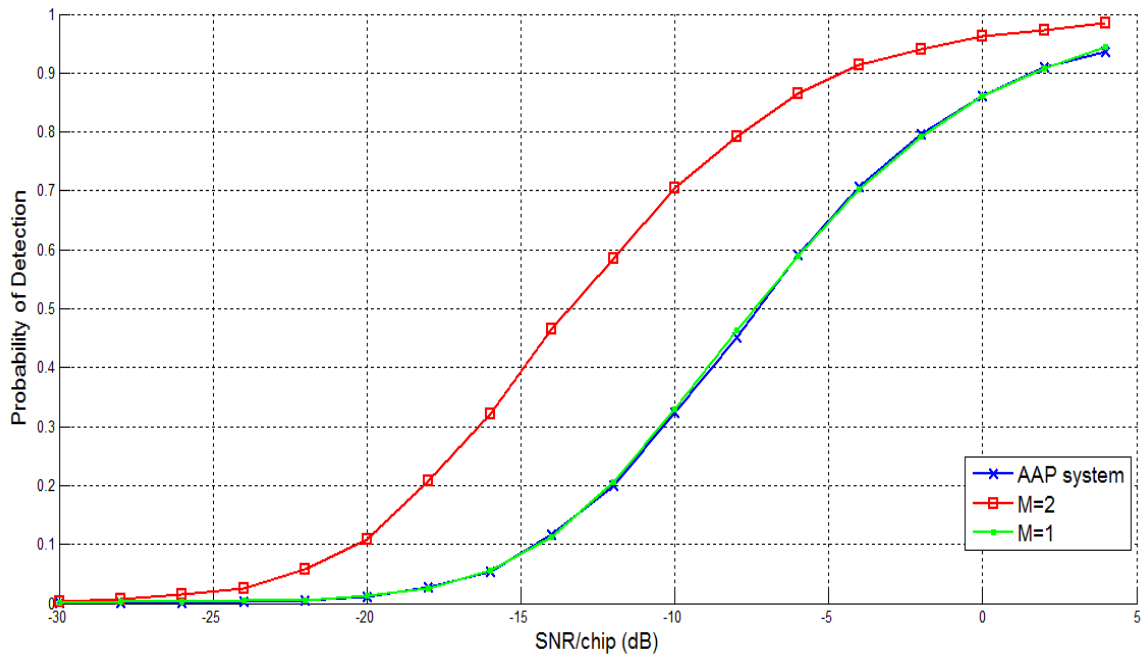


Fig. 3-9: Comparison of P_d between the proposed system with $M = 1$ and 2 and the APP system.

We observe that both systems have equivalent detection performance when $M = 1$. However, once we have two antenna elements, the detection performance is seriously improved, which shows clearly the effect of employing a smart antenna with more than one antenna elements in increasing the received signal power and thereby improving the detection performance.

In the Fig. 3-10, the detection performance is shown for $M = 2, 3, 4, 5$ and 6 antenna elements. Three interfering signals are assumed present and censored before the computation of the adaptive threshold. As expected, the detection performance improves significantly as the number of antenna elements increases. This is due to the nature of smart antenna which has the capability of improving signal power gain,

combating MAI signals, and reducing multipath fading as mentioned earlier. We also observe that as the number of antenna elements becomes greater than $M = 4$, we start reaching saturation.

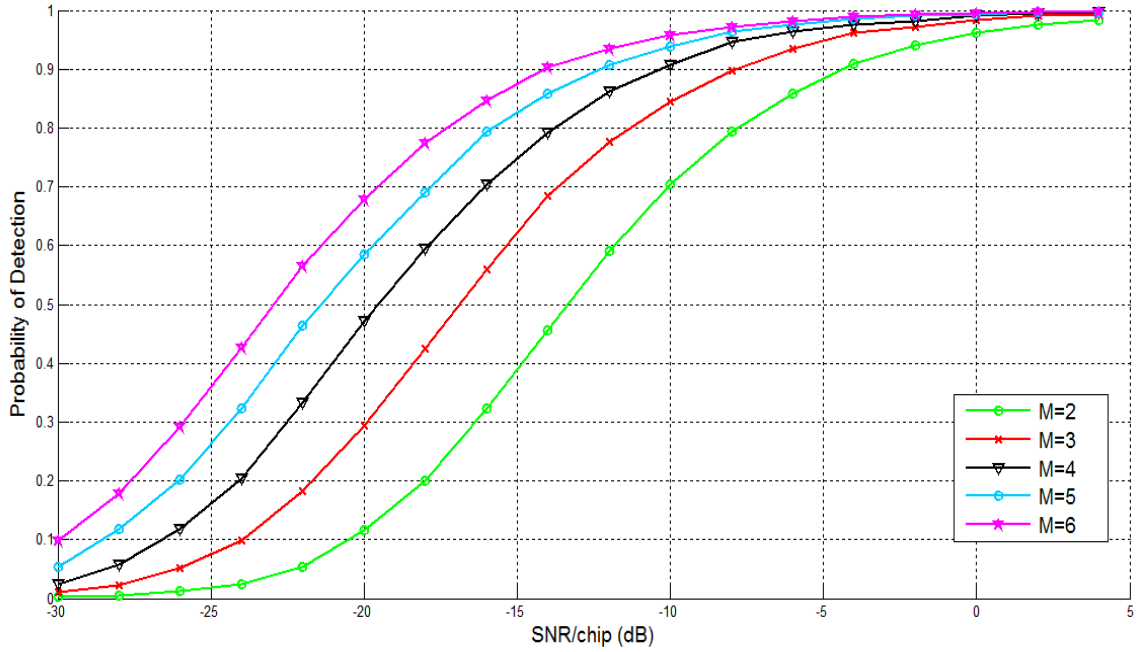


Fig. 3-10: Effect of the number of antenna elements M on the detection performance.

Fig. 3-11 shows the detection probabilities P_d of the proposed system with different number of antenna elements and for different numbers of censored cells. The number of antenna elements in the first system is $M = 2$, while in the second system is $M = 5$. The number of interfering signals is three with $\beta = 0.3$. We observe that as the number of antenna elements increases, the probability of detection improves as expected. It should be noted though that the detection performance in the presence of two interfering signals when $M = 5$ and $k = 1$, is better than the case with $M = 2$ and $k = 3$ case, which is the case with no interfering signals, and for all $SNR/chip$ values. We also observe a capture effect on the detection probability as it cannot reach $P_d = 1$

without censoring and this for all interfering signals. This emphasizes the robustness of the censoring algorithm which allows the probability of detection to reach asymptotically one as the $SNR/chip$ increases.

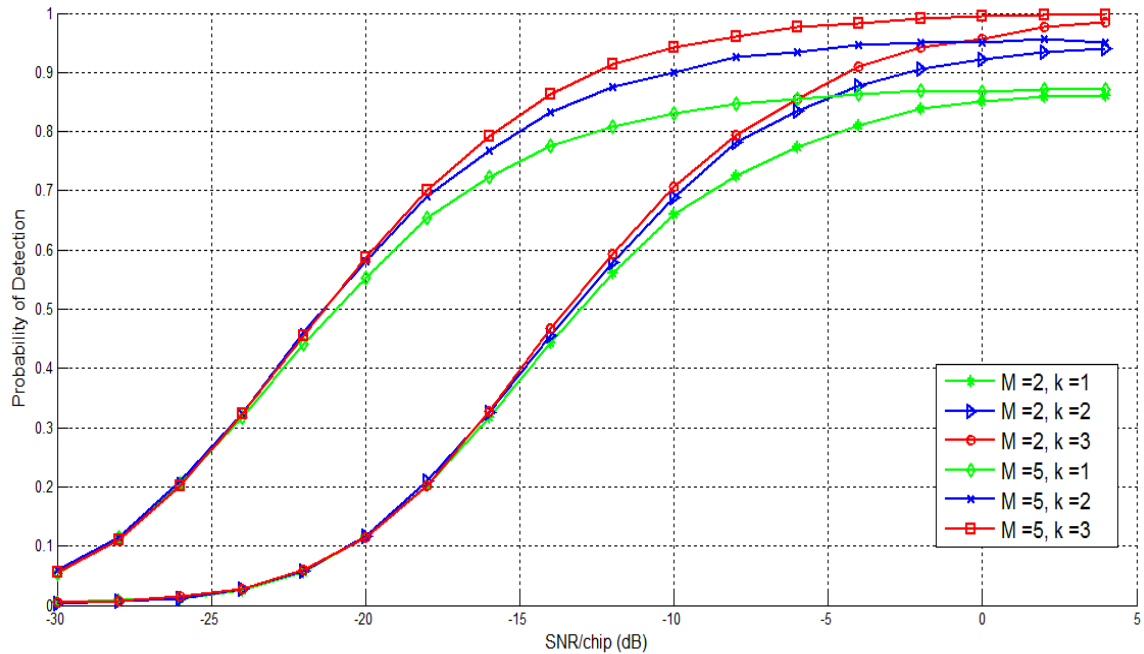


Fig. 3-11: Comparison of P_d for different number of antenna elements M and different values of number of censored cells k .

To evaluate the effect of the reference window size on the probability of detection, we show in Fig. 3-12 a plot of P_d against $SNR/chip$ for different number of reference cells $N_c = 16, 24$ and 32 with different number of antenna elements $M = 3$ and 5 . Three interfering signals are assumed to be present and censored before the computation of the adaptive threshold. As expected, increasing the window size N_c increases the detection probability as it gives estimate of the noise power in the cell under test. On the other hand, we observe that the probability of detection for the same number of reference cells is substantial increased when the number of antenna elements

is increased from 3 to 5. This indicates that the effect of the number of the smart antenna elements on the received signal power is much more pronounced on the probability of detection than the number of cells used in estimating the noise power. It also justifies the idea of combining both adaptive thresholding based on order statistics and censoring of interfering signals, and smart antenna.

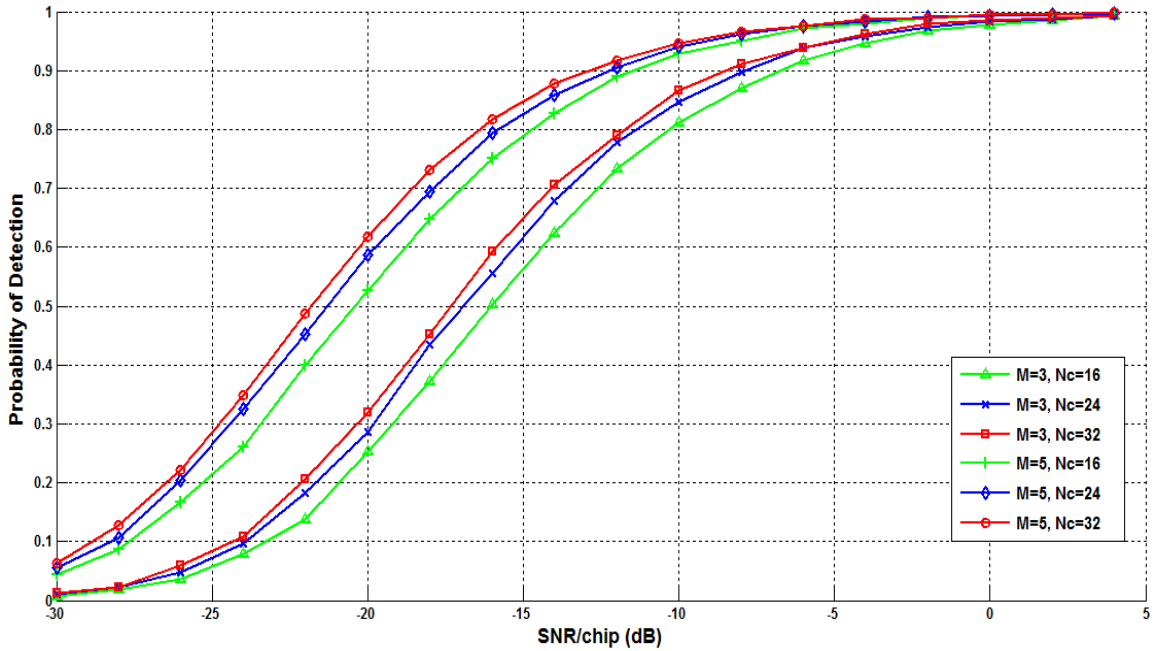


Fig. 3-12: Effect of the number of reference cells N_c on the detection performance.

To investigate the effect of the correlation length integer R on the probability of detection, a plot of P_d against $SNR/chip$ for different values of R ($R = 128, 256$, and 512) is shown in Fig. 3-13. The number of reference cells is $N_c = 24$, the number of antenna elements is $M = 2$, and three cells are assumed to have interfering signals which are censored before the computation of the adaptive threshold. We observe that increasing the correlation length integer R enhance the detection performance.

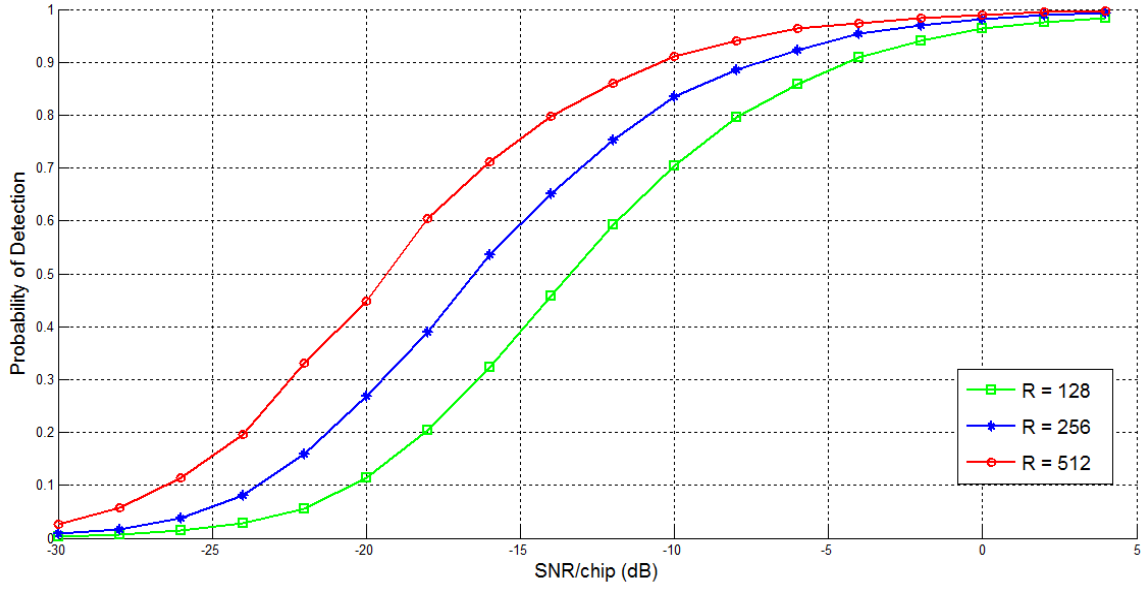


Fig. 3-13: Effect of the correlation length integer R on the detection performance.

3.4.2 Mean Acquisition Time

In this section, the mean acquisition time T_{acq} of the proposed system is evaluated. We consider a PN code sequence of length 1023 chips with a rate of 1 Mchips/sec . Consequently, the length of the uncertainty region for the serial search mode is 2046 test positions. The probability of false alarm is set to $P_{fa} = 10^{-3}$ and the penalty time factor $p = 1000$. The correlation length integer of the dwell time interval is set at value $R = 128$ and the number of reference cells is $N_c = 24$ unless otherwise stated. In Fig. 3-14, we plot T_{acq} against $SNR/chip$ for different number of antenna elements $M = 1, 2, 3$ and 4. The number of received multipath signals is two and three multipath cells are assumed to be in the reference window, which are censored before the computation of the adaptive threshold. The figure shows that as the number of antenna elements increase, T_{acq} decreases. We also observe a large improvement in T_{acq} from the single antenna element case.

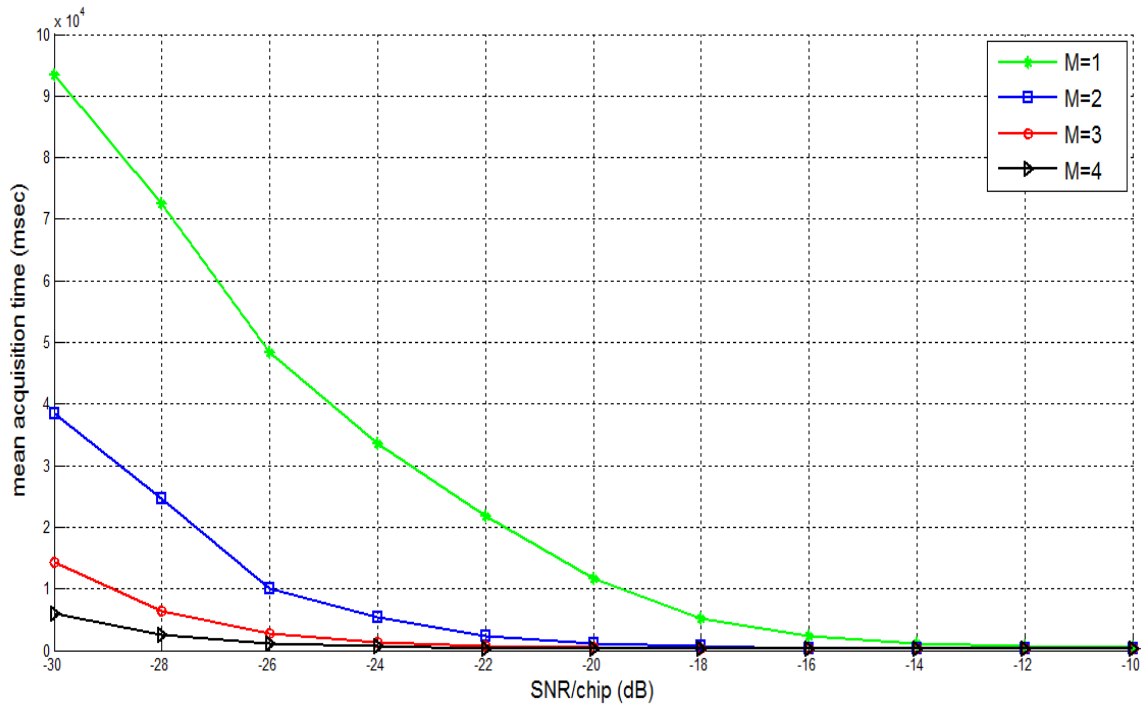


Fig. 3-14: Effect of the number of antenna elements M on the T_{acq} .

Under same conditions and for a system that use two antenna elements, the effect of increasing the correlation length integer on the mean acquisition time is shown in Fig. 3-15. As the R increase from 128 to 256 and 512, T_{acq} decreases. We note the sensitivity of T_{acq} decrease as the correlation length R increases and the $SNR/chip$ increases.

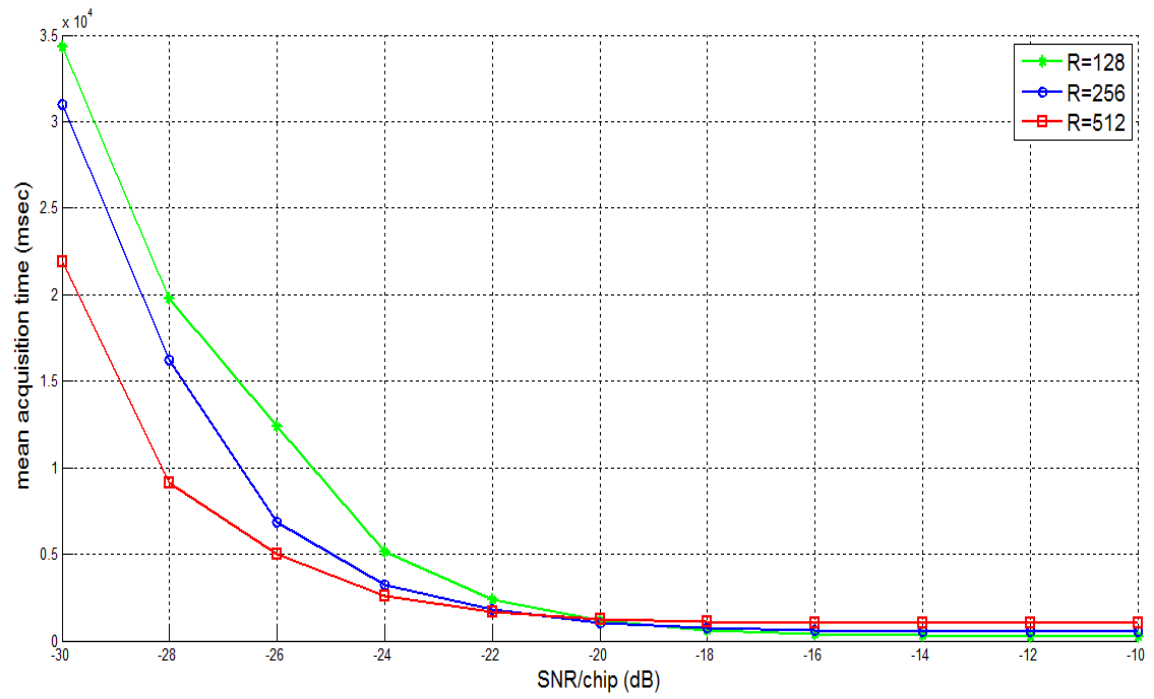


Fig. 3-15: Effect of the correlation length integer R on T_{acq} .

Chapter 4

Conclusion

Summary

In this chapter, a summary of the research work is given with some conclusions drawn from the obtained results. Some suggestions for future research work will be made.

4.1 Summary and Conclusions

4.2 Suggestions for Future Work

4.1 Summary and Conclusions

Efficient PN code acquisition is a significant requirement for wireless wideband DS-SS-CDMA communication receivers. Achieving a reliable PN acquisition in today's varying mobile environments in the presence of multipath and MAI signals is a challenge. That is, acquiring the PN code sequence both quickly and accurately is an important requirement for high quality communication.

In this thesis, we considered an efficient adaptive single dwell serial PN code acquisition scheme for a wideband wireless communication system that uses smart antenna and adaptive thresholding CMLD-CFAR detection in a Rayleigh slowly fading multipath communication channel. The signal is received by all antenna elements of a smart antenna. The smart antenna uses an iterative adaptive LMS algorithm to adjust its weight for better signal reception of the desired signal while minimizing the effect of multipath and interferences. Then a synchronization cell decision is made based on adaptive thresholding CFAR processing. We derived closed form expressions for the probability of false alarm, the probability of detection, and the mean acquisition time for the wideband communication system considered. Then we investigated the performance of the system in terms of PN acquisition in a Rayleigh slowly fading multipath channel. The effect of employing all antenna elements of the smart antenna, the detection, and the mean acquisition time on the PN acquisition performances have been studied in terms of computer simulations under different design parameters.

We have shown that employing all smart antenna elements improved the detection performance and the mean acquisition time of the PN code acquisition. We have also shown that increasing the window size and the correlation length integer improve the detection performance. The mean acquisition time was found to decrease as the

correlation length integer increased. Hence, the simulation results presented showed the robustness of the proposed communication system with smart antenna and adaptive thresholding CFAR processing for wideband communication in a Rayleigh slowly fading multipath channel.

4.2 Suggestions for Future Research Work

It is evident from the results obtained that employing adaptive CMLD CFAR processing with smart antennas in spread spectrum communication improves the PN code acquisition performance in Rayleigh slowly fading multipath communication channels compared to the CA-CFAR. The proposed wireless communication system for PN code acquisition can be further investigated with different CFAR processors and for other PN code acquisition search mechanisms.

Appendix

MATLAB Codes

Summary

In this appendix we present the MATLAB codes that are used to obtain the simulation results.

- 1. MATLAB Code for the Function of the Probability of False Alarm.**
- 2. MATLAB Code for the Simulation of the Probability of Detection.**
- 3. MATLAB Code for the Simulation of the Mean Acquisition Time.**

1. MATLAB Code for the Function of the Probability of False Alarm

```
% ===== %
% The function of the probability of false alarm equation
% ===== %

function Pfa = RT_Pfa_CMLD (Thresh, Nc, k)

% This function return the probability of false alarm Pfa
% based on the equation 3-21
%
%INPUTS
% Thresh    is the threshold multiplier
% Nc        is the reference window size
% k         is the number of censored cells
%

% create a matrix to store the moment generation function MGF
MgfV=repmat(0,1,Nc-k);

% to compute the MGF of the V's random variables
for i=1:(Nc-k)
    if i==1
        MgfV1=(Nc./((Nc-k).*(Thresh + (Nc./(Nc-k)))));
        MgfV(i)=MgfV1;
    end
    if i>=2
        MgfVi=((Nc-i+1)./(Nc-k-i+1))./(((Nc-i+1)./(Nc-k-
i+1))+Thresh);
        MgfV(i)=MgfVi;
    end
end

% the Pfa is the product of the MGF's
Pfa=prod(MgfV);
end
```

2. MATLAB Code for the Simulation of the Probability of Detection.

```
% ===== %
% The simulation of detection probability
% ===== %
%
% this code for computing the simulated probability of
% detection

clear;
clc;

%
% Simulation Parameters
%

Nc = 24; % number of cells in the reference window
Pfa = 10^-3; % the design Pfa
noI=3; % the number of interfering signals, it is assumed to
be known
k= 3; % number of censored cells
R=512; % the correlation length integer
M=2; % number of antenna elements
beta=0.3; %represents the average received power of the
           %interfering signal to the signal power of the
           %first user ratio

% To get the threshold multiplier T for the design Pfa using
the Pfa equation

f=@(T) (Pfa - RT_Pfa_CMLD(T, Nc, k));
T=fzero(f, [-1, 100]);

SNRdb=[-30:2:5]; % for plotting in db
runs=10000; %number of runs for each SNR value

for i=1:length(SNRdb) % for a range of SNR value for the CUT

H1_count=0; % counter of H1
SNR(i)=(10^(SNRdb(i)/10))* 0.5625*R*M;
I= beta*SNR(i);

    for j=1:runs %for each SNR value a 10,000 run will be
                % made to compute the Pd
```

```

% 1- add the interference samples in the reference window
    interf_samples = exprnd(M*(1+(M*I)),1,noI);%generate it
    window_samples(1:noI)= interf_samples; % add it to the
window

    % 2- add the noise only samples in the reference window
    noise_samples=exprnd(M,1,Nc-noI); % generate it
    window_samples(noI+1:Nc)= noise_samples; % add it to the
window

    % order the content of the window
    window_samples = sort(window_samples);

    %the reference window after censoring from the upper end
    window_samples = window_samples(1:Nc-k);

    % transform the contents to iid R.V.
    ref_win(1)= (Nc-k)*window_samples(1);
    for w=2:Nc-k
        ref_win(w)=(Nc-k-w+1)*(window_samples(w)-
window_samples(w-1));
    end

    U=sum(ref_win); % the estimate of noise level
    Z=T*U; % the adaptive threshold

    % the CUT under the H1 assumption
    CUT = exprnd(M*(1+(M*SNR(i))),1,1);

    if CUT>Z % compare the CUT with the threshold
        H1_count=H1_count+1;
    end
end
end
Pd(i)=H1_count/runs; % the Pd
end

%for plotting graph
hold on;
grid on;
plot(SNRdb,Pd,'-*r')
xlabel(['SNR/chip (dB)'], 'FontSize', 14)
ylabel(['Probability of Detection'], 'FontSize', 14);

```

3. MATLAB Code for the Simulation of the Mean Acquisition Time.

```
% ===== %
% The simulation of mean acquisition time MAT
% ===== %
%
% this code for computing the MAT of the simulated Pd

clear;
clc;

%
% Simulation Parameters
%

Nc = 24; % number of cells in the reference window
Pfa = 10^-3; % the design Pfa
noI=3; % the number of interfering signals, it is assumed to
be known
k= 3; % number of censored cells
R=128; % the correlation length integer
M=2; % number of antenna elements
beta=0.5; %represents the average received power of the
          % interfering signal to the signal power of the
          % first user ratio

% the following is the parameters of the MAT
L=2; % number of multipaths in the uncertainty region
N=2*L; % number of H1 cells in the H1 collective state
PN_U_chips= 1023; % the PN length is assumed to be 1023
chips
%the number of chips in the uncertainty region is assumed to
be all PN chips
q=2*PN_U_chips; %number of code phases to be tested is 2046
v=1+(q-N); % number of states in the flow graph
penalty=1000; % penalty factor
PN_chip_rate= 1*10^6; % the chip rate is set to 1 Mega chips
per one sec
Tc=1/PN_chip_rate; % chip time
dwell_time = R*Tc; % dwell time

% to get the threshold multiplier value for the design Pfa
f=@(T) (Pfa - RT_Pfa_CMLD(T, Nc,k));
T=fzero(f,[-0.5, 100]);
```

```

SNRdb=[-30:2:-10]; % for plotting in db

runs=10000; %number of runs for each SNR value

for i=1:length(SNRdb) % for a range of SNR value for the CUT
    H1_count=0; % counter of H1
    SNR(i)=(10^(SNRdb(i)/10))* 0.5625*R*M;
    I= beta*SNR(i);

    for j=1:runs %for each SNR value a 10,000 run will be
        % made to compute the Pd

        % 1- add the interference samples in the reference window
        interf_samples = exprnd(M*(1+(M*I)),1,noI); % generate it
        window_samples(1:noI)= interf_samples; % add it to the window

        % 2- add the noise only samples in the reference window
        noise_samples=exprnd(M,1,Nc-noI); % generate it
        window_samples(noI+1:Nc)= noise_samples; % add it to the
        window

        % order the content of the window
        window_samples = sort(window_samples);

        % the reference window after censoring from the upper end
        window_samples = window_samples(1:Nc-k);

        % transforms the contents to iid R.V.
        ref_win(1)= (Nc-k)*window_samples(1);
        for w=2:Nc-k
            ref_win(w)=(Nc-k-w+1)*(window_samples(w) -
            window_samples(w-1));
        end

        U=sum(ref_win); % the estimate of noise level
        Z=T*U; % the adaptive threshold

        % the CUT under the H1 assumption
        CUT = exprnd(M*(1+(M*SNR(i))),1,1);
    end
end

```

```

        if CUT>Z % compare the CUT with the threshold
            H1_count=H1_count+1;
        end
    end

    Pd(i)=H1_count/runs; % the Pd

% for computing the MAT
    signal =0;

    for jj=1:N
        fact=1;
        for ii=1:jj-1
            fact= fact*(1-Pd(i));
        end
        signal = signal+(jj*Pd(i)*fact);
    end

    Fact=1;
    for jj=1:N
        Fact= Fact*(1-Pd(i));
    end

    sigma2 =0;
    for jj=1:N
        fact=1;
        for ii=1:jj-1
            fact= fact*(1-Pd(i));
        end
        sigma2 = sigma2+(Pd(i)*fact);
    end

%Now the MAT is computed using the equation 3-36
    MAT(i) = ((2*signal + 2*N*Fact + (v-1)*(1+penalty*Pfa)*(2-
sigma2))/(2*sigma2))*dwell_time;
    MAT(i) = MAT(i)*10^3; % converting to ms
end

%for plotting graph
hold on;
grid on;
plot(SNRdb,MAT,'-*b')
xlabel(['SNR/chip (dB)'], 'FontSize', 14)
ylabel(['mean acquisition time (msec)'], 'FontSize',14);

```


References

- [1] A. Sofwan and M. Barkat, "PN code acquisition Using Smart antennas and adaptive thresholding trimmed-mean CFAR processing for CDMA communication," in *Spring World Congress on Engineering and Technology* (SCET2012), Xi'an, China, 2012.
- [2] W. Zhuang, "Noncoherent hybrid parallel PN code acquisition for CDMA mobile communications," *IEEE Transactions on Vehicular Technology*, vol. 45, pp. 643-656, 1996.
- [3] A. Polydoros and C. Weber, "A unified approach to serial search spread-spectrum code acquisition--Part I: General Theory," *IEEE Transactions on Communications*, vol. 32, pp. 542-549, 1984.
- [4] L.-L. Yang, and L. Hanzo, "Serial acquisition of DS-CDMA signals in multipath fading mobile channels," *IEEE Transactions on Vehicular Technology*, vol. 50, pp. 617-628, 2001.
- [5] E. A. Sourour and S. C. Gupta, "Direct-sequence spread-spectrum parallel acquisition in a fading mobile channel," *IEEE Transactions on Communications*, vol. 38, pp. 992-998, 1990.
- [6] R. R. Rick and L. B. Milstein, "Parallel acquisition in mobile DS-CDMA systems," *IEEE Transactions on Communications*, vol. 45, pp. 1466-1476, 1997.
- [7] A. Van Der Meer and R. Liyana-Pathirana, "Performance analysis of a hybrid acquisition system for DS spread spectrum," in *TENCON 2003. Conference on Convergent Technologies for Asia-Pacific Region*, vol.1, pp. 121-125, 2003.
- [8] M. Barkat, *Signal Detection and Estimation*, 2nd Edition, Artech House, Boston, MA. 2005.
- [9] C.-J. Kim, H.-J. Lee, and H.-S. Lee, "Adaptive acquisition of PN sequences for DSSS communications," *IEEE Transactions on Communications*, vol. 46, pp. 993-996, 1998.
- [10] H. M. Finn and R. S. Johnson, "Adaptive detection mode with threshold control as a function of spatially sampled clutter-level estimates," *RCA Review*, vol. 29, pp. 414-464, 1968.
- [11] H. Rohling, "Radar CFAR thresholding in clutter and multiple target situations," *IEEE Transactions on Aerospace and Electronic Systems*, vol. AES-19, pp. 608-621, 1983.
- [12] C. M. Cho and M. Barkat, "Moving ordered statistics CFAR detection for nonhomogeneous backgrounds", *IEEE Proceedings part F, Radar and Signal Processing*, vol. 140, pp.284-290, 1993.
- [13] J. T. Rickard and G. M. Dillard, "Adaptive detection algorithms for multiple-target situations," *IEEE Transactions on Aerospace and Electronic Systems*, vol. AES-13, pp. 338-343, 1977.

- [14] J. A. Ritcey, "Performance analysis of the censored mean-level detector," *IEEE Transactions on Aerospace and Electronic Systems*, vol. AES-22, pp. 443-454, 1986.
- [15] P. P. Gandhi and S. A. Kassam, "Analysis of CFAR processors in nonhomogeneous background," *IEEE Transactions on Aerospace and Electronic Systems*, vol. 24, pp. 427-445, 1988.
- [16] M. Barkat, H. D. Himonas, and P. K. Varshney, "CFAR detection for multiple target situations", *IEE Proceedings, Part F, Radar and Signal Processing*, vol. 136, No. 5, pp. 193-210, 1989.
- [17] S. D. Himonas and M. Barkat, "Automatic censored CFAR detection for nonhomogeneous environments", *IEEE Transactions on Aerospace and Electronic Systems*, vol. AES-28, No. 1, pp. 286-304, 1992.
- [18] M. E. Smith and P. K. Varshney, "Intelligent CFAR processor based on data variability, " *IEEE Transactions on Aerospace and Electronic Systems*, vol. AES-36, No. 3, pp. 837-847, 2000.
- [19] A. Farrouki and M. Barkat, "Automatic censoring CFAR detector based on ordered data variability for nonhomogeneous environments", *IEE Proceedings, Radar Sonar and Navigation*, vol. 152, pp. 43-51, 2005
- [20] T.-T.V. Cao, "Constant false-alarm rate algorithm based on test cell information" *IET Radar Sonar and Navigation*, vol. 2, No. 3, pp. 200-213, 2008.
- [21] X.W. Meng, "Comments on constant false-alarm rate algorithm based on test cell information", *IET Radar Sonar and Navigation*, vol. 3, No. 6, pp. 646-649, 2009.
- [22] R. Zhang, W. Sheng, and X. Ma, "Improved switching CFAR detector for non-homogeneous environments", *Signal Processing*, vol. 93, pp. 35-48, 2013.
- [23] S. Erfanian and V. T. Vakili, "Introducing switching ordered statistics CFAR type I in different radar environments", *EURASIP Journal on Advances in Signal Processing*, vol. 2009, pp. 1-11, 2009.
- [24] J. J. Jen, *A study of CFAR implementation cost and performance tradeoffs in heterogeneous environments*, Master thesis, Department of electrical and computer engineering, California State Polytechnic University, Pomona, 2011
- [25] S. Benkrinah and M. Barkat, "An adaptive acquisition using order statistic CFAR in DS-CDMA serail search for a multipath Rayleigh fading channel", *Proceedings of the Third IEEE International Conference on Systems, Signals and devices*, Tunisia, 2005.
- [26] S. Benkrinah, M. Barkat, M. Benslama, A. Benmeddour, and R. Bekhakhecha, "Adaptive acquisition of PN sequence in nonfading AWGN channels", *African Physical Review*, vol. 2, pp. 120-122, 2008.
- [27] C.-J. Kim, "Adaptive acquisition of PN code in multipath fading mobile channels," *Electronics Letters*, vol. 38, pp. 135-137, 2002.
- [28] Y. Song and G. Hu, "Adaptive acquisition of PN code using excision CFAR detector in multipath fading mobile channels," *Electronics Letters*, vol. 40, pp. 338-339, 2004.

- [29] M. Barkat, "A modified CFAR detector", *Proceedings of the 22nd Annual Conference on Information Sciences and Systems*, Princeton University, New Jersey, pp. 605-610, 1988.
- [30] M. Katz, J. Linatti, and S. Glisic, "A comparative study of code acquisition using antenna diversity and beamforming techniques", *IEEE Seventh International Symposium on Spread Spectrum techniques and Applications*, vol. 1, pp. 223-227, 2002.
- [31] H. Krouma and M. Barkat, "An adaptive threshold double-dwell systems with antenna diversity for DS-CDMA acquisition", in *UAE Forum on Telecommunication Research*, Sharjah, UAE, 2006.
- [32] H. Krouma, M. Barkat, K. Kemih, M. Benslama, and Y. Yacine, "Performance analysis of an adaptive threshold hybrid double-dwell systems with antenna diversity for acquisition in DS-CDMA systems", *International Journal of Information Technology*, vol. 4, No.1, pp. 75-84, 2008.
- [33] H. Kwon, L. Song, S. Y. Kim, and S. Yoon, "Noncoherent constant false alarm rate schemes with receive diversity for code acquisition under homogeneous and nonhomogeneous fading circumstances", *IEEE Transactions on Vehicular Technology*, vol. 56, pp. 2108-2120, 2007.
- [34] R. Bekhakhecha, M. Barkat, and S. Alshebeili, "Adaptive acquisition of a PN code using OS-CFAR detection and antenna diversity for a multipath Rayleigh fading channel," in *International Conference on Computer and Communication Engineering*, Malaysia, 2006.
- [35] B. Wang and H. M. Kwon, "PN code acquisition using smart antenna for spread-spectrum wireless communications. I," *IEEE Transactions on Vehicular Technology*, vol. 52, pp. 142-149, 2003.
- [36] B. Wang and H. M. Kwon, "PN code acquisition for DS-CDMA systems employing smart antennas .II," *IEEE Transactions on Wireless Communications*, vol. 2, pp. 108-117, 2003.
- [37] H. Puska, H. Saarnisaari, J. Linatti, and P. Lilja "Serial search code acquisition using smart antennas with single correlator or matched filter," *IEEE Transactions on Communications*, vol. 56, pp. 299-308, 2008.
- [38] N. Alhariqi, M. Barkat and A. Sofwan, "Serial PN Acquisition Using Smart Antenna and Censored Mean Level CFAR Adaptive Thresholding for a DS/CDMA Mobile Communication," *Proceedings of the IEEE 14th International Conference on High Performance Computing and Communications (HPCC 2012)*, pp. 1193-1198, Liverpool, UK, June 2012.
- [39] K. S. Zigangirov, *Theory of Code Division Multiple Access Communication*, 1st Edition, Wiley-IEEE Press, 2004.
- [40] R. Pickholtz, D. L. Schilling, and L. B. Milstein, "Theory of Spread-Spectrum Communications--A Tutorial," *IEEE Transactions on Communications*, vol. 30, pp. 855-884, 1982.
- [41] D. Campana and P. Quinn, "Spread-spectrum communications," *IEEE Potentials*, vol. 12, pp. 13-16, 1993.
- [42] D. Prabakaran. (2005) Spread-Spectrum Technology and its Application, *Electronics for you*.

- [43] I. J. Meel, "Spread Spectrum (SS) introduction," De Nayer Institut, Belgium, 1999.
- [44] M. K. Simon, J. K. Omura, R. A. Scholtz, and B. K. Levitt, *Spread Spectrum Communications Handbook*, McGraw-Hill, 2002.
- [45] D. Torrieri, *Principles of Spread-Spectrum Communication Systems*, 1st Edition, Springer, Boston, 2005.
- [46] G. V. Trunk, "Range resolution of targets using automatic detection", *IEEE Transactions on Aerospace and Electronic Systems*, vol. AES-14, pp.750-755, 1978.
- [47] V. G. Hansen and J. H. Sawyers, "Detectability loss due to greatest of selection in a cell averaging CFAR", *IEEE Transactions on Aerospace and Electronic Systems*, vol. AES-16, pp.115-118, 1980.
- [48] P. H. Lehne and M. Pettersen, "an overview of smart antenna technology for mobile communications systems," *IEEE Communications Surveys*, vol. 2, 1999.
- [49] S. Bellofiore, C. A. Balanis, J. Foutz, and A. S. Spanias "Smart-antenna systems for mobile communication networks. Part 1. Overview and antenna design," *IEEE Antennas and Propagation Magazine*, vol. 44, pp. 145-154, 2002.
- [50] I. Stevanović, A. Skrivervik and J. R. Mosig, "Smart Antenna Systems for Mobile Communications," 2003.
- [51] C. A. Balanis and P. I. Ioannides, *Introduction to Smart Antennas*, 1st Edition, Morgan & Claypool, 2007.
- [52] A. O. Boukalov and S. G. Haggman, "System aspects of smart-antenna technology in cellular wireless communications-an overview," *IEEE Transactions on Microwave Theory and Techniques*, vol. 48, pp. 919-929, 2000.
- [53] R. K. Jain, S. Kativar, and N. K. Agrawal "Smart Antenna for Cellular Mobile Communication," *VSRD International Journal of Electrical, Electronics & Communication Engineering*, vol. 1, pp. 530-541, 2011.
- [54] C.-J. Kim, T.-W. Hwang, H.-J. Lee, and H.-S. Lee, "Acquisition of PN code with adaptive threshold for DS/SS communications", *Electronics Letters*, vol.33, no.16, pp.1352-1354, 1997 .
- [55] Y. S. Song, H. M. Kwon, and B. J. Min, "Computationally efficient smart antennas for CDMA wireless communications", *IEEE Transactions on Vehicular Technology*, vol. 50, pp.1613-1238, 2000.
- [56] H. A. David and H. N. Nagaraja, *Order Statistics*, 3rd Edition, Wiley, New Jersey, 2003.
- [57] U. Kamps and U. Gather, "Characteristic Properties of Generalized Order Statistics From Exponential Distributions ", *Applicaciones Mathematicae*, pp.383-391, 1997.